β-cell response to high fat diet induced metabolic demands

in the obese Wistar rat

by

Candice Rene Roux

Thesis presented in partial fulfilment of the requirements for the degree
Master of Science in Medical Sciences
at the University of Stellenbosch

Supervisor: Dr. Christo John Frederick Muller
Co-supervisors: Prof. Benedict Page and Dr. Marlon Eugene Cerf
Faculty of Health Sciences
Department of Biomedical Sciences

March 2011

DECLARATION

By submitting this thesis/dissertation electronically, I declare that the entirety of the work contained therein is my own, original work, that I am the sole author thereof (save to the extent explicitly otherwise stated), that reproduction and publication thereof by Stellenbosch University will not infringe any third party rights and that I have not previously in its entirety or in part submitted it for obtaining any qualification.

March 2011

ABSTRACT

Introduction: A westernized diet rich in saturated fats and sugars, together with a sedentary lifestyle, has contributed to the dramatic increase in obesity during the last decade (Zimmett *et al,* 2001; Wild *et al,* 2004). Obesity is associated with dyslipidemia and insulin resistance which are major risk factors for the development of type 2 diabetes (T2D) (Zimmet *et al*, 2001, Kahn *et al*, 2006; Schröder *et al*, 2007). High-fat feeding in rodents induces symptoms similar to the human metabolic syndrome without progression to T2D (Woods *et al*, 2002; Weir and Bonner-Weir, 2007). The addition of fructose to a high-fat diet exacerbates the insulin resistance and leads to impaired pancreatic function of insulin secretion and glucose intolerance (Basciano *et* al, 2005; Stanhope *et al*, 2009).

Aims: The aim of this study was to establish the effect of a high-fat and sucrose/fructose diet on glucose metabolism, the development of insulin resistance and β-cell dynamics.

Methods: Weanling Wistar rats were randomized into two study groups; study one over an experimental period for three months and study two for twelve months. Each study consisted of a control group that received standard rat chow and water; and two experimental groups receiving either a high-fat diet and water (HFD) or a café diet consisting of HFD with the addition of 15% sucrose/fructose (CFD). Fasting glucose and insulin concentrations, intravenous glucose tolerance test (IVGTT), glucose stimulated insulin secretion rates and 2-deoxy-[^{3}H]-D-glucose uptake in muscle, liver and fat were measured. The pancreata were harvested for immunohistochemical labeling of β-cells (insulin), α-cells (glucagon), GLUT2 (glucose transport) and MIB5 (proliferation). Samples of the pancreata were also collected for electron microscopy.

Results and discussion: Feeding Wistar rats a CFD induced obesity, insulin resistance and glucose intolerance. By twelve months the rats had an impaired glucose response with increased IVGTT peak values, area under the curve (AUC) values and glucose clearance rates. Concomitantly, the glucose stimulated insulin secretion rate (GS-ISR) was attenuated. Stimulated glucose disposal as measured by 2-deoxy-[^{3}H]-D-glucose uptake was reduced in muscle and adipose tissue at three months. By twelve months, due to the age of the rats, stimulated glucose uptake declined compared to three months with no difference between groups. After three months the diets had no observable effect on the islets using light microscopy. However, by twelve months morphological changes were observed in both the HFD and CFD groups. In the HFD group large hypertrophied irregular islets with fibrous changes were observed. In the CFD group these morphological changes were more prominent with fibrous segregation and disruption of the normal endocrine arrangement. In addition, the presence of inflammatory cells within the affected islets is consistent with T2D.

Conclusion: High-fat diet fed to Wistar rats induced obesity, abdominal adiposity and insulin resistance. The addition of sucrose/fructose to a high-fat diet exacerbated the insulin resistance and resulted in glucose intolerance and mild hyperglycemia. Morphological changes in the large islets were observed which are consistent with the development of T2D.

ABSTRAK

Inleiding: ‘n Verwesterde dieët, ryk aan versadigde vette en suikers tesame met ‘n passiewe lewenstyl, het bygedra tot die dramatiese verhoging in vetsug gedurende die laaste dekade (Zimmett *et al,* 2001; Wild *et al,* 2004). Vetsug word met dislipidemie en insulienweerstandigheid geassosieer wat hoof risikofaktore is vir die ontwikkeling van tipe 2 diabetes (T2D) (Zimmet *et al*, 2001; Kahn *et al*, 2006; Schröder *et al*, 2007). Hoë-vet voeding in knaagdiere induseer simptome soortgelyk aan menslike metaboliese sindroom sonder die ontwikkeling van T2D (Woods *et al*, 2002; Weir and Bonner-Weir, 2007). Die byvoeging van fruktose tot ‘n hoë-vet dieët vererger insulienweerstandigheid en lei tot verswakte pankreas funksie, insuliensekresie en glukoseintoleransie (Basciano *et* al, 2005; Stanhope *et al*, 2009).

Doelwitte: Die doelwitte van die studie was om die effek van hoë-vet en sukrose/fruktose voeding op glukosemetabolisme, die ontwikkeling van insulienweerstandigheid en β-sel dinamika te bepaal.

Metodes: Gespeende Wistar rotte was in twee groepe gerandomiseer; studie een oor ’n tydperk van drie maande en studie twee oor ’n tydperk van twaalf maande onderskeidelik. Elke studie het ‘n kontrole groep met standard rot kos en water (control); en twee experimentele dieëte wat of ’n hoë-vet dieët en water (HFD) of ‘n kafeedieët groep wat die HFD met die byvoeging van 15% sukrose/fruktose in hul drink water (CFD) ontvang. Fastende glukose and insulien, binneaarse glukose toleransie toets (IVGTT), glukose gestimuleerde insulien sekresie tempo en 2-deoxi-[^{3}H]-D-glukose opname in spier, lewer en vet is gebruik om die effek van die dieët op glukosemetabolisme te bepaal. Die pankreata is uitgehaal vir immunohistochemiese identifisering van β-selle (insulien), α-selle (glukagoon), GLUT2 (glukose transport) en MIB5 (proliferasie). Monsters van die pankreata was ook vir elektronmikroskopie versamel.

Resultate en bespreking: Voeding van ’n CFD aan Wistar rotte induseer vetsug, insulienweerstandigheid en glukose-intoleransie Teen twaalf maande toon die rotte ‘n verswakte response tot glukose met verhoogde IVGTT piekwaardes, AUC waardes en glukose opriumingswaardes. Tenselfdetyd is die glukose gestimuleerde insuliensekresie tempo (GS-ISR) ook verswak. Gestimuleerded glukose opruiming, soos deur 2-deoxi-[^{3}H]-D-glukose opname bepaal, was verlaag in spier en vetweefsel teen drie maande. Teen twaalf maande, weens die ouderdom van die rotte, is die gestimuleerde glucose opname verlaag in vergelyking met drie maande sonder ‘n verskil tussen groepe. Na drie maande kon geen sigbare morfologiese verskille met ligmikroskopie tussen die dieëte waargeneem word nie. Teen twaalf maande is morfologiese verskille waargeneem in beide die HFD en die CFD groepe. In die HFD groep is groot hipertrofiese onreëlmatige eilande met fibrotiese verandering waargeneem. In die CFD groep was die morfologiese verandering meer gevorder met fibrotiese onderverdeling en ontwrigting van die normale endokriene rangskikking. Die teenwoordigheid van inflammatoriese selle in die geaffekteerde eilande is verenigbaar met T2D.

Afleiding: Die voer van ‘n hoë-vet dieët aan Wistar rotte veroorsaak vetsug, abdominale adipositeit en insulienweerstandigheid. Die byvoeging van sukrose/ fruktose tot die hoë-vet dieët vergerger die insulienweerstandigheid en veroorsaak glukoseintoleransie en matige hiperglukemie. Morfologiese veranderings in die groter eilande was verenigbaar met T2D.

ACKNOWLEDGEMENTS

I would like to thank the following people for their contribution and assistance during this study:

My supervisor Dr. Christo Muller for his profound assistance, guidance, scientific knowledge and endless encouragement.

My co-supervisors, Prof. Ben Page and Dr. Marlon Cerf for scientific contributions.

Dr. Johan Louw, Platform director of Diabetes Discovery Platform, for allowing me the opportunity to study further and for approving financial support from the Medical Research Council. Also for having kind words and understanding throughout my studies.

All my colleagues at Diabetes Discovery Platform, for technical assistance and proof reading. Special thanks to Nireshni and Samira for all the support and encouragement.

Mrs. Nolan Muller at Diagnostic electron microscopy unit, NHLS, Tygerberg Hospital for assistance with electron microscopy.

Primate Unit staff at the Medical Research Council for the housekeeping and maintenance of the rats during the study and for the use of facilities.

My family, especially my parents and Nabeal for their unconditional love, support and encouragement.

Wish to thank God for granting me the abilities to complete this project.

TABLE OF CONTENTS

LIST OF FIGURES

LIST OF TABLES

LIST OF ABBREVIATIONS

^{3}H	tritium
ADA	American Diabetes Association
ADP	adenosine diphosphate
APES	3-aminopropyltriethoxy-silane
ATP	adenosine triphosphate
AUC	area under the curve
BMI	body mass index
Ca^{2+}	calcium
CFD	café diet
cpm	counts per minute
CVD	cardio-vascular diseases
DAB	diaminobenzidine tetrachloride
DIO	diet-induced obesity
dpm	disintegrations per minute
Fc region	fragment crystallizable region
FFA	free fatty acid
fINS	fasting serum insulin
fPG	fasting plasma glucose
GCR	glucose clearance rate
GLUT2	glucose transporter 2
GLUT4	glucose transporter 4
GS-ISR	glucose stimulated insulin secretion rate
H_2O_2	hydrogen peroxide

HDL	high density lipoprotein
HFCS	high-fructose corn syrup
HFD	high-fat diet
HOMA-IR	homeostatic model assessment of insulin resistance
IAPP	islet amyloid poly peptide
Ig	immunoglobulins
IHC	immunohistochemistry
IL-1	interleukin 1
IL-6	interleukin-6
IRS1	insulin receptor substrate one
IRS2	insulin receptor substrate two
IVGTT	intravenous glucose tolerance test
K^+	potassium
KOH	potassium hydroxide
LDL	low density lipoprotein
min	minutes
NGS	normal goat serum
NHS	normal horse serum
RF	retroperitoneal fat
RGB	red, green, blue
RIA	radioimmunoassay
rpm	revolutions per minute
SOP's	standard operating procedures
T2D	type 2 diabetes

TBS	tri(hydroxymethyl)-aminomethane buffered saline
TNFα	tumor necrosis factor alpha
Tris	tri(hydroxymethyl)-aminomethane
WHO	World Health Organization
ELISA	enzyme-linked immunosorbent assay

INTRODUCTION

The incidence of obesity has risen to alarming levels, with an estimate of 300 million people affected worldwide (Schröder *et al*, 2007). In addition the prevalence of diabetes has also increased dramatically, with an estimate of 150 million people in 2000, likely to double by 2025. This places a huge burden on available health resources especially in developing countries (Prentki and Nolan, 2006; Schröder *et al*, 2007). A close relationship exists between obesity, the development of metabolic syndrome and T2D (Zimmet *et al*, 2001; Schröder *et al*, 2007). A westernized lifestyle and diet with high saturated fat content has been shown to be the main contributing factors to increasing obesity, developing insulin resistance and T2D (Zimmet *et al*, 2001; Cerf, 2007; Thévenod, 2008).

In order to maintain normoglycemia, due to increased body mass, the body compensates by hypersecretion of insulin and increased insulin synthesis resulting in increased β-cell mass (Prentki and Nolan, 2006). The larger demand for insulin eventually results in β-cell dysfunction and loss of β-cells due to apoptosis (Butler *et al*, 2003).

High-fat feeding of rats, not genetically predisposed to developing diabetes, induces obesity and insulin resistance without the progression to T2D (Woods *et al*, 2002; Weir and Bonner-Weir, 2007). The addition of sucrose/fructose exacerbates the effect of high-fat feeding by increasing dyslipidemia, further decreasing insulin sensitivity and increasing visceral adiposity (Basciano *et* al, 2005; Stanhope *et al*, 2009).

CHAPTER ONE

LITERATURE REVIEW

1.1 The pancreas and β-cells

The pancreas is a digestive organ that produces and secretes digestive fluids containing various digestive enzymes via its exocrine acinar cells and ducts. It contains endocrine cells that appear as discrete cell clusters called islets containing a heterogeneous population of neuroendocrine cells which produce four major hormones namely insulin (secreted by the β-cells), glucagon (secreted by the α-cells), somatostatin (secreted by the δ-cells) and pancreatic poly-peptide (PP-cells) (Ganong, 1989; Stevens and Lowe, 2005). Insulin and glucagon have important functions in the metabolism of carbohydrates, proteins and fats and plays a major role in maintenance of glucose homeostasis (Ganong, 1989).

In 1939 H.P. Himsworth observed that certain patients were more sensitive to the hypoglycemic effect of insulin than others that required higher doses of insulin (Reaven, 2005). These observations were the first reference to the concept of impaired insulin action or insulin resistance (Reaven, 2005) which is a crucial factor in the development and pathogenesis of T2D (WHO, 2006)

1.2 Obesity

Obesity is defined as an excessive accumulation of body fat to an extent where it may have adverse effects on the health of the individual (WHO, 2006; Galic *et al*, 2010). The cause of obesity is a prolonged imbalance where energy intake levels exceed energy expenditure which results in lipids being stored as excess fat (Speakman *et al*, 2007). According to the WHO, obesity is defined as a body mass index (BMI) equal to or more than 30 kg/m^2 (WHO, 2006). Body mass index is calculated as the weight in kilograms divided by the square root of the height in meters of an individual.

Worldwide, the prevalence of obesity has risen to alarming levels, with approximately 300

million people affected (Schröder, 2007). The WHO projects that approximately 2.3 billion adults will be overweight and more than 700 million adults will be obese in 2015 (WHO, 2006).

In developing countries, including South Africa, a migration from a traditional rural to a westernized diet is associated with an increased consumption of energy-dense foods containing refined carbohydrates, sugars and high saturated fats (Cerf, 2007). A general decline in physical activity further leads to an increase in body mass (Schröder *et al*, 2007). A close relationship exists between obesity and the development of T2D with the common cause being unhealthy diets (Schröder, 2007) and sedentary lifestyle (Zimmet *et al,* 2001).

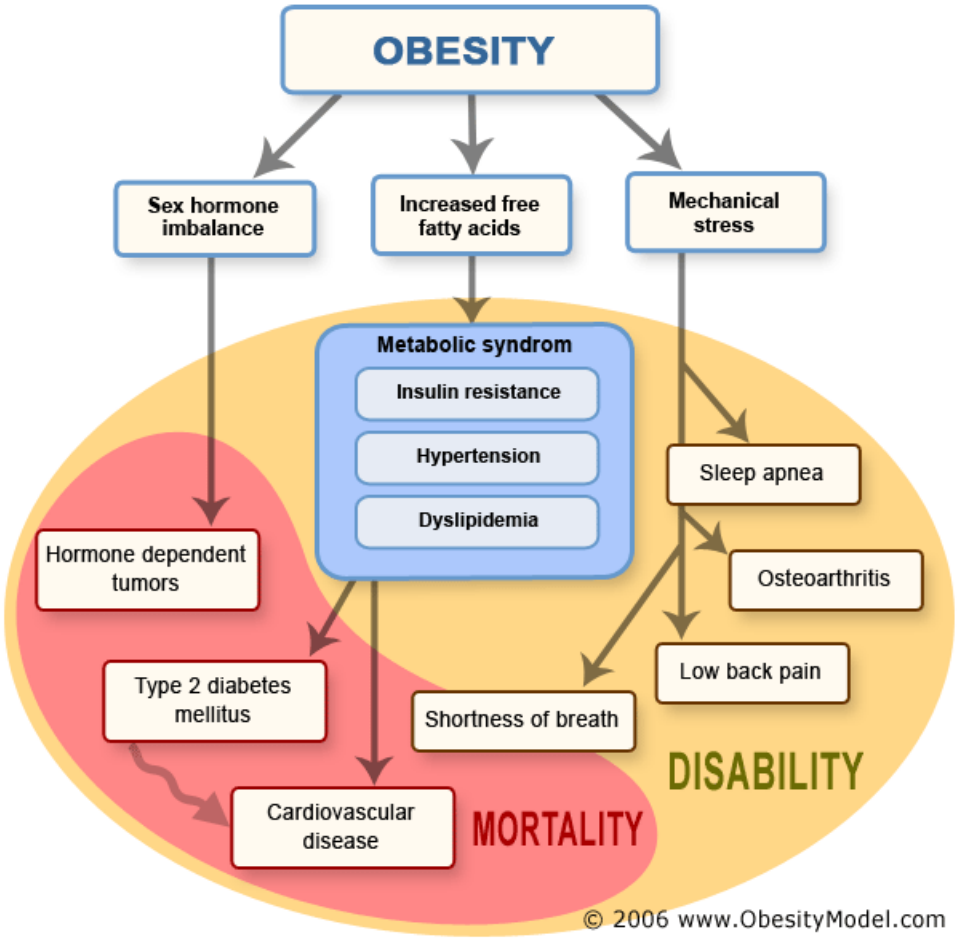

Figure 1: Schematic diagram depicting the adverse effects of obesity

Several other adverse health consequences of obesity (Fig 1) include insulin resistance, coronary heart disease, hypertension, fetal defects due to maternal obesity and certain types of cancers such as endometrial, breast (in postmenstrual woman) and colon (WHO, 2000). The accumulation of lipids in adipose tissue plays an important role in the regulation of fatty acid metabolism where in periods of calorie abundance it stores free fatty acid (FFA) as triglycerides and can therefore release them into the circulation when there is a shortage of energy (Galic *et al*, 2010). The increased storage of fatty acids in expanded adipose tissue mass is closely related to the development of insulin resistance in insulin sensitive tissues such as skeletal muscle and liver (Galic *et al*, 2010).

The relationship between a diet with high saturated fat content and obesity, insulin resistance and T2D is well established (Zimmet *et al*, 2001; Cerf, 2007; Thévenod, 2008). In the young and adult populations, the increase in the consumption of fructose has been identified as a major cause of obesity. The consumption of fructose with a high-fat diet synergistically exacerbates insulin resistance and dyslipidemia (Basciano *et al*, 2005).

Many genetic and diet-induced obesity (DIO) animal models have been developed to study the physiology and genetic basis of obesity. Diet-induced obesity in animal models using high-fat feeding closely resembles the human development of the metabolic syndrome (Buettner *et al*, 2006). In non-genetic predisposed rodents the extent of obesity depends on the specific rodent strain in combination with the diet regime followed. High-fat fed Wistar rats and C57BL/6J mice develop obesity and insulin resistance while 129S6 and A/J mice do not (Buettner *et al*, 2006).

In the genetically pre-disposed leptin deficient obese mouse (*ob/ob*) the mutation generates massive obesity. This defect results in a premature stop codon in the gene expressed almost exclusively in adipocytes (Speakman *et al*, 2007; Galic *et al*, 2010). Leptin has been

identified as a signal of adipose tissue storage; in obesity leptin concentrations are increased (Galic *et al*, 2010).

1.3 Metabolic syndrome (Syndrome X)

The concept of Syndrome X, first introduced in the Banting Lecture 1988 (Reaven, 1988), included individuals that were insulin resistant, compensatory hyperinsulinemic, glucose intolerant and exhibited increased plasma triglycerides and decreased high density lipoprotein (HDL) cholesterol. The name Syndrome X originates from the algebraic term, the letter X which equals the unknown because the association between insulin resistance and the association with its risk factors for cardio-vascular diseases (CVD) was unknown (Reaven, 2005). The term Syndrome X has been replaced by insulin resistance syndrome which describes an array of abnormal and clinical syndromes associated with insulin resistance (Fig 2) (Reaven, 2005).

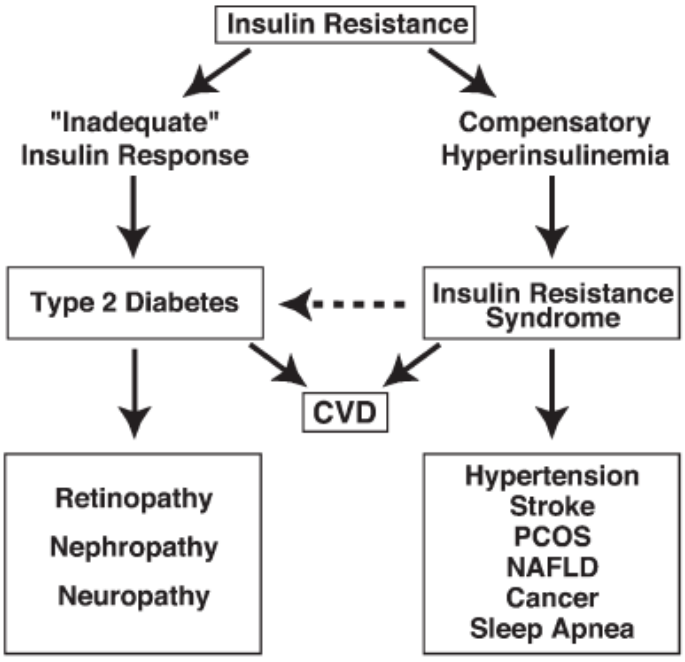

Figure 2: Schematic diagram depicting the manifestations of the Insulin Resistance Syndrome (Reaven, 2005)

The metabolic syndrome comprises a cluster of metabolic disorders which includes increased body mass, abdominal obesity, insulin resistance, hyperglycemia, dyslipidaemia and hypertension (Pittas *et al*, 2004; Després and Lemieux, 2006; Fulop *et al,* 2006; Azevedo *et al,* 2009). These are all risk factors for the development of T2D and CVD and are all major causes of morbidity and mortality (Azevedo *et al,* 2009).

Abdominal obesity is the major determinant and most prevalent manifestation of the metabolic syndrome (Després and Lemieux, 2006; Fulop *et al,* 2006; Monteiro and Azevedo, 2010). The increase in abdominal obesity leads to adipocyte hypertrophy which causes these cells to rupture and evoke an inflammatory response (Fulop *et al,* 2006; Monteiro and Azevedo, 2010) which results in a chronic low-grade inflammation (Boden, 2006). Inflammation is driven by adipokines and cytokines (Fig 3) secreted by these hypertrophic, adipocytes and macrophages respectively (Fulop *et al*, 2006). Visceral adipose tissue in particular is able to secrete adipokines with endocrine, paracrine and autocrine activity able to induce insulin resistance, inflammation, dyslipidemia and endothelial dysfunction (Fulop *et al*, 2006). Some adipokines e.g. adiponectin, has protective effects against the development of metabolic syndrome (Fulop *et al*, 2006).

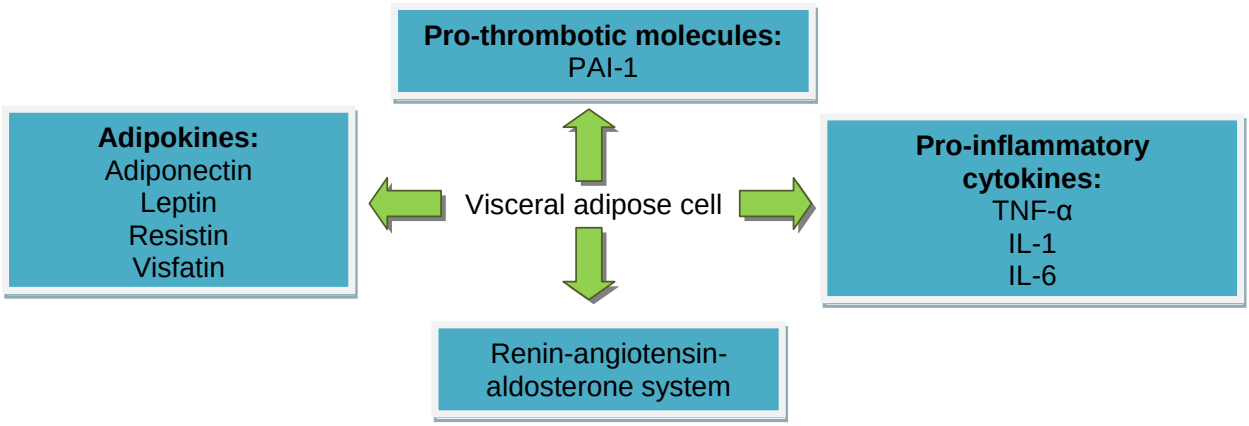

Figure 3: Obesity mediated inflammatory response (Adapted from Fulop *et al*, 2006)

Excess fat deposition in other vital organs, such as the liver, has severe consequences on insulin resistance (Monteiro and Azevedo, 2010). The anatomic distribution of adipose tissue potentially has a major effect on insulin sensitivity. The accumulation of abdominal visceral fat correlates strongly with the development of insulin resistance (Fulop *et al*, 2006). In contrast, subcutaneous adipose tissue, which has a large fat storage capacity, acts as a reservoir and has a protective effect against the development of metabolic syndrome (Monteiro and Azevedo, 2010). Viscerally obese individuals represent a sub-group with severe insulin resistance. Insulin resistant, visceral adipocytes cause increased release of FFA from the visceral tissue to the liver resulting in lipoprotein and lipid metabolism disturbances (Fulop *et al*, 2006). This leads to liver insulin resistance, glucose intolerance, increased triglycerides and LDL- cholesterol which are common features of viscerally obese individuals. In addition to its fat storage function, adipose tissue can be regarded as an endocrine organ due to its ability to release adipocyte-specific factors such as adipokines (Galic *et al*, 2010). In addition to adipokines, the visceral adipocytes and or infiltrating macrophages secrete pro-inflammatory cytokines of which tumor necrosis factor α (TNFα) is the most important. TNFα modulates the expression of leptin and interleukin- 6 (IL-6) while suppressing adiponectin thereby linking visceral obesity with insulin resistance and metabolic syndrome (Fulop *et al*, 2006).

1.4 Insulin Signaling

Insulin is a peptide hormone secreted in response to increased circulating glucose levels by the β-cell in the pancreas (Pessin and Saltiel, 2000; Chakraborty, 2006). Insulin is essential in regulating carbohydrate, lipid and protein metabolism and the maintenance of whole-body glucose homeostasis (Pessin and Saltiel, 2000; Chakraborty, 2006; Sesti, 2006). Insulin

induces increased lipid synthesis in the liver and fat cells and decreases lipolysis from triglycerides in fat and muscle tissue (Chakraborty, 2006).

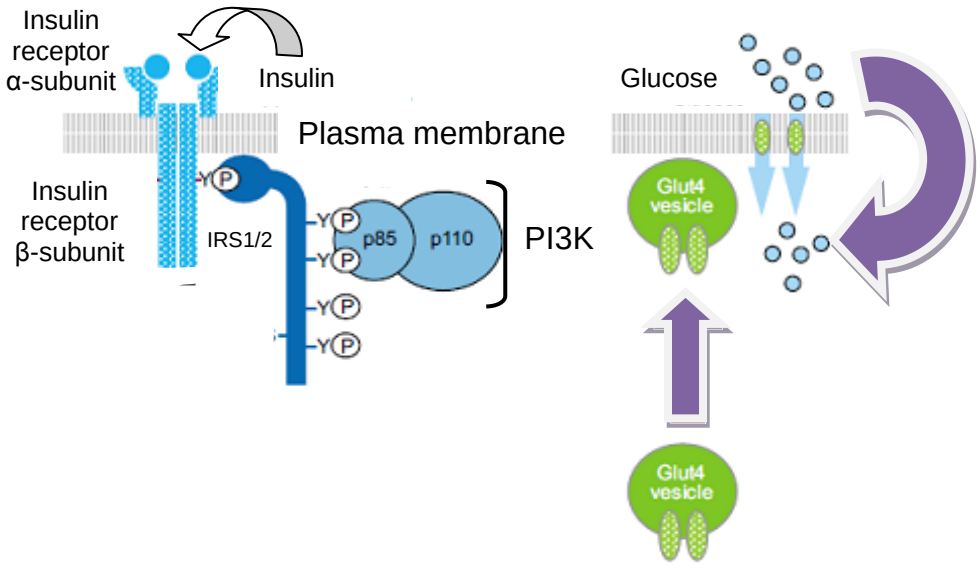

Figure 4: Insulin signaling pathway (Adapted from Choi and Kim, 2010)

Insulin-stimulated glucose uptake in muscle and fat is initiated by the binding of insulin to the insulin receptor (α-subunit) on the cell surface, resulting in autophosphorylation of multiple tyrosine residues of the insulin receptor β-subunit in the cytoplasm (Fig 4). This results in tyrosine phosphorylation of insulin receptor substrates (IRS1 and IRS2). Phosphorylation of the IRS proteins facilitates the binding of Src homology 2 (SH2) domain (p85 subunit) of phosphoinositide 3-kinase (PI3K). Activation of PI3K initiates the PI3K/Akt pathway which results in glucose transporter four (GLUT4) translocation from a cytoplasmic pool to the plasma membrane. Glucose is then actively transported into the cell via GLUT4 located in the plasma membrane.

The PI3K/Akt pathway plays a pivotal role in insulin signaling and glucose transport via GLUT4. In T2D, PI3K activity decreases in skeletal muscle providing evidence that deficient insulin signaling could result in impaired GLUT4 mediated glucose transport and insulin resistance (Choi and Kim, 2010). Similarly Akt in muscle from non-obese T2D while Akt2 phosphorylation is impaired from adipocytes in obese type 2 diabetics (Choi and Kim, 2010).

Increased concentrations of FFA, directly or in combination, with inflammatory cytokines e.g TNF-α cause several defects in insulin signaling (Griffin *et al*, 1999; Yu *et al*, 2002). Resulting in serine phosphorylation, instead of tyrosine phosphorylation, of IRS1. This causes IRS protein degradation or IRS protein inhibiting the activation of the PI3K/Akt pathway (Yu *et al*, 2002; Sesti, 2006). Therefore GLUT4 translocation is inhibited and glucose transport into the cell is attenuated (Sesti, 2006).

1.5 Insulin Resistance

Insulin resistance is defined as the inability of target organs, liver, muscle and fat tissues, to respond effectively to insulin stimulation (Pittas *et al*, 2004; Chakraborty, 2006). Therefore during the development of insulin resistance the body compensates by increasing insulin secretion (Pittas *et al*, 2004). To compensate for the ever increasing demand for insulin, pancreatic β-cell mass increases either by β-cell hypertrophy or β-cell hyperplasia (Weir and Bonner-Weir, 2007; Fujitani *et al*, 2010). The balance between islet β-cell hypertrophy, β-cell proliferation and β-cell apoptosis directly determines β-cell mass (Weir *et al*, 2001). The capacity of the functional β-cell mass to increase in response to insulin resistance is crucial to prevent the development of T2D (Weir and Bonner-Weir, 2007). A fundamental aspect of the pathogenesis of diabetes is the failure of the pancreatic β-cells to synthesize and secrete sufficient amounts of insulin to maintain normoglycemia (Weir *et al*, 2001).

The assessment of insulin resistance using HOMA-IR is a tool commonly used for a crude measurement of insulin resistance (Bonora *et al,* 2002). It is less invasive, inexpensive therefore a more efficient way of assessing insulin resistance when compared to glucose clamp tests (Kang *et al*, 2005). HOMA-IR limitations are to be considered especially in subjects with low BMI, low β-cell function, high fasting glucose concentrations in T2D patients (Kang *et al*, 2005) and older people (Chang *et al*, 2006).

1.6 β-cell mass and dynamics

There are four major mechanisms involved in the regulation of β-cells mass i.e. neogenesis, size modification, replication and apoptosis (Dor *et al*, 2004; Halban, 2004; Bonner-Weir *et al*, 2005; Rhodes, 2005; Marchetti *et al*, 2008). β-cell mass is represented by the sum of neogenesis, replication and size minus the rate of apoptosis at any given time (Rhodes, 2005; Marchetti *et al*, 2008; Karaca *et al*, 2009).

A key issue in the understanding of the pathogenesis of diabetes is the regulation of β-cell mass (Bouwens and Rooman, 2005). At birth, the number of β-cells present is mainly generated by proliferation and differentiation of pancreatic progenitor cells through neogenesis (Bouwens and Rooman, 2005; Rhodes, 2005; de Koning, 2008; Marchetti *et al*, 2008). After birth, a proportion of cycling β-cells can expand in cell number to compensate for an increased insulin demand mainly by β-cell proliferation and to a lesser extent by β-cell neogenesis (Bouwens and Rooman, 2005). β-cell proliferation is increased and the rate of apoptosis is low which creates the increased β-cell growth early in life. These growth mechanisms adjust during childhood and adolescence which creates equilibrium of sufficient β-cell mass thought adulthood (Marchetti *et al*, 2008). With aging, the β-cell mass decreases

as the rate of apoptosis outweigh proliferation (Rhodes, 2005; Marchetti *et al*, 2008). This could explain why the elderly are more prone to develop T2D (Rhodes, 2005).

The lifespan of β-cells in rodents is estimated at approximately 60 days with approximately 0.5% of adult β-cells undergoing apoptosis (Rhodes, 2005). Normally the resultant loss of β-cells is compensated by β-cell replication (Rhodes, 2005). β-cell failure occurs when the critical β-cell mass declines to such an extent that the remaining β-cells are unable to compensate for the insulin requirements (Prentki *et al*, 2006). The most likely mechanisms involved in early β-cell mass reduction includes mitochondrial dysfunction, oxidative stress, endoplasmic reticulum stress, dysfunctional triglycerides, FFA and glucolipotoxicity (Prentki *et al*, 2006). The subsequent development of hyperglycemia includes additional processes linked to glucotoxicity including islet inflammation, O-linked glycosylation and amyloid deposition that accelerates β-cell apoptosis (Prentki *et al*, 2006). Amylin (islet amyloid poly-peptide- IAPP) co-secreted with insulin, has been implicated in β-cell failure and is the pre-curser of amyloid deposition in T2D (DeFronzo, 2004). Elevated plasma IAPP levels have been associated with T2D patients, obese glucose intolerant subjects and in animal models of diabetes (DeFronzo, 2004). It is suggested that elevated levels of FFA and amylin hypersecretion as is found in insulin resistance acts synergistically to impair β-cell function and cause β-cell injury (DeFronzo, 2004).

Glucotoxicity is associated with hyperglycemia that causes β-cell desensitization to glucose and increased apoptosis (Marchetti *et al*, 2008). Clinical evidence has proven that lowered serum glucose concentrations in T2D patients can cause an increase in their acute insulin response to glucose (Marchetti *et al*, 2008). Glucotoxicity is associated with inflammatory cytokines, like interleukin one beta (IL-1β), secreted by human islets, in the presence of high

glucose concentrations which can mediate β-cell apoptosis (Maedler *et al*, 2002).

In insulin resistant and T2D patients, dyslipidemia and resultant lipotoxicity, associated with the accumulation of FFA and their metabolic products have a deleterious effect on β-cells (Maedler *et al*, 2002). In addition lipotoxicity alters insulin signaling in the liver and skeletal muscle thereby contributing to whole body insulin resistance and deterioration of glucose tolerance (Galgani *et al*, 2008). A study inducing glucolipotoxicity in Wistar rats caused insulin resistance at six months but not in two month old rats which suggests that older animals should be used in studies of diet induced insulin resistance and which closely mimic typical T2D (Fontés *et al*, 2010).

1.7 Diet-induced type 2 diabetic animal models

Animal models in the study of diabetes are advantageous and offer useful insights into the mechanisms of human diabetes (Srinivasan and Ramarao, 2007). Rodent models fed a high-fat diet have contributed significantly to our understanding of the pathophysiology of insulin resistance. According to Buettner *et al*, the first description of a high-fat diet used to induce obesity via nutritional intervention was performed by Masek and Fabry in 1959 (Buettner *et al*, 2006). Different types of fat in high-fat diets have varying effects on glucose metabolism in Wistar rats. Lard, rich in polyunsaturated fatty acids, and olive oil, rich in monounsaturated fatty acids, as the main fat components has shown the most pronounced manifestations of obesity and insulin resistance when compared to coconut fat and fish oil (Buettner *et al*, 2006). These results suggest that the accepted hypothesis that all saturated fatty acids exacerbates insulin resistance, needs further study (Buettner *et al*, 2006). In the short term (a three to four week intervention), high polyunsaturated diet feeding induced insulin resistance without hyperglycemia in Wistar rats (Chalkley *et al*, 2002). Similarly, Wistar rats fed a

safflower oil-based high-fat diet (59% calories as fat) from two months old for a ten months period, developed insulin resistance but not diabetes (Chalkley *et al*, 2002). It suggested that without a genetic predisposition, the high-fat feeding alone does not result in T2D (Chalkley *et al*, 2002). A study by Krygsman *et al* showed that not only the percentage dietary fat that plays a role in glucose intolerance and insulin resistance but a relationship between fatty acid composition and dietary fat (Krygsman *et al*, 2010).

High-fructose corn syrup (HFCS), as sweetener, is commonly used in food especially beverages, including carbonated sodas (Hofmann and Tschöp, 2009). The use of HFCS has been proposed as an important dietary factor that has contributed to the widespread increase in human obesity observed in Westernized societies (Hofmann and Tschöp, 2009). HFCS contains 5% more fructose compared to sucrose ("normal sugar"). Fructose exerts an increased perception of sweetness therefore it is preferred by food and soft drink manufacturers (Hofmann and Tschöp, 2009).

The addition of fructose to a high-fat diet is commonly used to induce an animal model of T2D (Huang *et al*, 2004). A study done by Huang *et al* concluded that a high-fructose diet causes hyperinsulinemia, while a high-fat diet results in impaired pancreatic function of insulin secretion and glucose intolerance this suggest that high-fructose diet and high-fat diet exerts divergent effects on glucose metabolism in rats (Huang *et al*, 2004). Relevant differences in metabolism of rats fed fructose-enriched diets showed substantial insulin resistance and hyperinsulinemia in both lean and obese rats, whereas rats fed a glucose-enriched diet led to enhanced insulin sensitivity (Suga *et al*, 2000). The metabolism of these sugars where comprehensively compared in overweight/obese humans and found that visceral adipose

volume was significantly increased in subjects consuming fructose (Stanhope and Havel, 2009) when compared to glucose consumption (Stanhope *et al*, 2009). Fasting plasma glucose and insulin concentrations increased and insulin sensitivity decreased in subjects consuming fructose but not those consuming glucose (Stanhope *et al*, 2009). High-fructose diets induce dyslipidemia, decrease insulin sensitivity and increase visceral adiposity (Stanhope *et al*, 2009).

1.8 Diabetes

Diabetes is defined as a chronic disease involving the β-cells in the pancreatic islets. In diabetes, β-cells cannot produce sufficient insulin or the body cannot efficiently utilize the insulin that is being produced (Zimmett, 2001; WHO, 2009). Diabetes is also associated with micro-vascular (retinopathy, nephropathy and neuropathy) and macro-vascular (ischemic heart disease, stroke and peripheral vascular disease) complications which generally reduces quality of life, life expectancy and increases morbidity (Zimmet *et al*, 2001; Roglic *et al,* 2006). Uncontrolled diabetes is characterized by hyperglycemia that over time is detrimental to many body systems (WHO, 2009). The recent increase in the incidence of diabetes is due to many factors including urbanization, diet, obesity and a sedentary lifestyle (Zimmett *et al,* 2001; Wild *et al,* 2004).

According to the WHO more than 220 million people worldwide have diabetes and an estimated 1.1 million people died from diabetes in 2005. Projections indicate that deaths attributed to diabetes will double from 2005 to 2030 (WHO, 2009).

The two main forms of diabetes are type 1 diabetes and T2D. Type 1 diabetes is an auto-immune disease that is characterized by destruction of pancreatic β-cells and leads to

deficient insulin secretion. Type 1 diabetes patients require exogenous insulin administration to control hyperglycemia (Zimmett *et al,* 2001; WHO, 2009). Type 2 diabetes is associated with obesity and sedentary lifestyle and accounts for 90% of people with diabetes (Zimmett *et al,* 2001; WHO, 2009). According to a review by DeFronzo, 2004, the pathophysiology of T2D starts with normal glucose tolerance, insulin resistance, compensatory hyperinsulinemia, with a progression to impaired glucose intolerance and T2D. The primary defects responsible for the progression to T2D is impaired insulin secretion by the β-cells, increased glucose production by the liver and decreased utilization of glucose by peripheral tissue such as muscle (DeFronzo, 2010). These phenomenons have been observed in many diverse populations and in animal models such as the rhesus monkey, which closely resembles T2D in humans (DeFronzo, 2004). Such studies have revealed a strong association between obesity and the development of T2D (Freemantle *et al*, 2008). A decrease in tissue insulin sensitivity with a compensatory increase in fasting and glucose-stimulated plasma concentrations is the earliest detectable abnormality that exists before the onset of diabetes (DeFronzo, 2004). When the rate of insulin secretion cannot be maintained any longer due to β-cell failure and loss of β-cell mass, fasting hyperglycemia and glucose intolerance follows which leads to the progression to T2D (DeFronzo, 2004).

During ingestion of a mixed meal, approximately 50% of glucose is used by the brain, 25% in splanchnic area (liver and gastrointestinal tissues) and the remaining 25% in muscle and to a lesser extent in adipose tissue (DeFronzo, 2004). During ingestion of glucose there is an increase in plasma glucose concentrations which then in turn stimulates the release of insulin by the pancreatic islets to dispose of excess glucose (DeFronzo, 2004). This causes a temporary state of hyperinsulinemia and hyperglycemia which stimulates glucose uptake by the splanchnic and muscle tissues (DeFronzo, 2004). A small amount (approximately 4-5%)

of glucose is metabolized by adipocytes, although it plays a major part in maintenance of total body glucose disposal by the regulation of FFA from stored triglycerides (DeFronzo, 2004). Increased insulin concentrations inhibit lipolysis and cause a decline in plasma FFA concentration, resulting in an increase in muscle glucose uptake. Insulin also suppresses glucose production in the liver (DeFronzo, 2004).

1.9 Glucose sensing and insulin secretion

Glucose transporter 2 (GLUT2) is a facilitative transporter of glucose, fructose and other dietary sugars, allowing bidirectional glucose flux and serves as an equilibrator of intra- and extra-cellular glucose concentrations, essential to the maintenance of glucose homeostasis (Leturque *et al*, 2005; Leturque *et al*, 2009). GLUT2 is located in the plasma membrane of liver, pancreas, kidneys, intestines and brain (Thorens *et al*, 2000; Leturque *et al*, 2005; Leturque *et al*, 2009). GLUT2 is able to process high concentrations of sugars mainly due to its low-affinity and high-capacity allowing fast equilibration of glucose (Kellett and Brot-Laroche, 2005; Leturque *et al*, 2005; Kramer *et al*, 2009; Leturque *et al*, 2009). In the rat it is also the main bidirectional glucose transporter in the liver (Leturque *et al*, 2005). In the presence of high glucose and insulin concentrations, the liver stores glucose as glycogen or metabolizes it to lipids. In the fasted state, glucagon stimulates glycogen degradation (glycogenolysis) where glycogen is converted to glucose-6-phosphate which is then hydrolyzed to glucose. Glucose is then exported from the cell via GLUT2 (Leturque *et al*, 2005). Transport of glucose via GLUT2 is the initial event of glucose-induced insulin secretion by the pancreatic β-cells and plays a key role in glucose sensing (Leturque *et al*, 2005; Cerf, 2007). The intra-cellular glucose is metabolized by glycolysis in the mitochondria in the β-cells. This triggers the distal step of insulin secretion where adenosine triphosphate

(ATP) to adenosine diphosphate (ADP) ratio controls the ATP-dependant-potassium (K^+) channel closure, causing membrane depolarization and opening of the voltage-dependent calcium (Ca^{2+}) channels. This increases intra-cellular Ca^{2+} and facilitates the release of secretory granules of insulin (Leturque *et al*, 2005; Cerf, 2007; Leturque *et al*, 2009). The secretion of insulin thereby stimulates the uptake of glucose in liver, skeletal and adipose tissue (Cerf, 2007).

Human studies have revealed that mutations in the GLUT2 gene causes Fanconi-Bickel syndrome which is an autosomal recessive disorder of carbohydrate metabolism (Santer *et al*, 1998; Bouché *et al*, 2004; Leturque *et al*, 2005). Patients with this disorder suffer from hepatomegaly, nephropathy, fasting hypoglycemia, glucose intolerance and growth retardation (Santer *et al*, 1998; Bouché *et al*, 2004; Leturque *et al*, 2005). They are unable to tolerate simple sugars in their diets (Santer *et al*, 1998; Bouché *et al*, 2004; Leturque *et al*, 2005).

Studies in GLUT2-null mice, unable to survive past the first three weeks of life (Thorens *et al*, 2000), can be maintained alive by insulin injections (Leturque *et al*, 2005). Suggesting that in mice no alternative pathway can restore glucose entry and insulin secretion (Leturque *et al*, 2005). These mice present with glucosuria indicating GLUT2 is essential in renal glucose reabsorption (Thorens *et al*, 2000; Leturque *et al*, 2005). GLUT2-null mice are hyperglucagonemic (Thorens *et al*, 2000) having a 40% larger liver than their controls due to accumulation of excess glycogen (Leturque *et al*, 2005).

Importantly, in humans a lack of GLUT2 in the pancreatic islets does not alter insulin secretion, as in mice (Leturque *et al*, 2005). Humans have a fourfold lower level of GLUT2

than mice pancreatic β-cells (Leturque *et al*, 2005) as the major transporter of glucose is glucose transporter one (GLUT1) (Zuniga *et al*, 2001). Glucose sensing plays a crucial role in pancreatic β-cells and impairment of glucose sensing contributes to β-cells dysfunction in rats (Cerf, 2007). A defect in GLUT2 sensing, leads to the inability of the pancreatic β-cells to sense changes in glucose can therefore be directly linked to the development of T2D in mice (Thorens, 2001).

1.10 Aim of the study

- To establish the effect of a high-fat and sucrose/fructose feeding on the glucose metabolism.
- The development of insulin resistance and β-cell mass dynamics and β-cell function in response to the dietary insult.
- To assess β-cell glucose transport by the expression of GLUT2.

CHAPTER TWO

MATERIALS AND METHODS

2.1 Animal model and housing

Wistar rats were used and bred at the Medical Research Council (MRC), Primate Unit, Tygerberg, South Africa. Rats were cared for and managed according to documented standard operating procedures (SOP) of the Primate Unit (De Villiers, 2007) and in accordance with the MRC Guidelines for the Use of Animals in Research and Training and the National Code for Animal Use in Research. Ethical approval for this study was obtained from the ethics committee at the Medical Research Council of South Africa (ECRA # 10/09).

After weaning, male Wistar rats (three week old) were placed and maintained on three different experimental diets for either three or twelve months. Rats were individually caged on sterilized absorbent corn cob bedding (Cobtech, Harrismith, SA) to ensure comfort. Clean cages and bedding were provided weekly. The rats had access to clean drinking water at all times. The rats were maintained in a temperature controlled room of 24 – 26 °C, humidity of 45 – 55%, 15 -20 air changes per hour and on a 12 hour light/dark cycle.

2.2 Experimental diet composition and calorific content

Three experimental diets varying in fat and carbohydrate content were designed for the study. The diets were designed to maintain similar protein content of approximately 15% only varying fat and carbohydrate content. The reason being that protein deficiency can lead to defects in insulin signaling (Araujo *et al*, 2004). The standard rat chow consisted of dry pellets and the high-fat diet, produced by the Primate Unit, consisted of a moist patty.

The macro-nutrient and calorific content is listed in Table 1.

Table 1: Dietary composition of the diets

Nutrients		Control	HFD	CFD
% Energy	Protein	15.13	15.09	15.09
	Fat	10.69	40.17	40.17
	Saturated (SFA)	3.98	18.27	18.27
	Monounsaturated (MUFA)	2.92	11.45	11.45
	Polyunsaturated (PUFA)	2.24	5.75	5.75
	Carbohydrate	74.16	44.73	44.73
Refined sugar:(99.98% carbohydrate) 7.5% sucrose: 7.5% fructose		0.00	0.00	15.00
Kcal/g of food		2.60	2.06	2.06
Kcal/g of sucrose/fructose		n/a	n/a	0.60
Total Kcal/g of diet		2.60	2.06	2.66

2.3 Experimental design

At three weeks of age, weanling male Wistar rats were randomized into two experimental study periods of three groups each (n= 60):

2.3.1 Study 1 (Three months diet groups):

Control diet group received standard maintenance rat chow (Atlas Animal Feed, Cape Town) and water *ad libitum* (n= 10). High-fat diet (HFD) fed group received HFD and water *ad libitum* (n= 10). Café diet (CFD) fed group received the HFD and 15% sucrose/fructose in drinking water *ad libitum* (n= 10). Diets were administered for three months.

2.3.2 Study 2 (Twelve months diet groups):

Control diet group received standard maintenance rat chow (Atlas Animal Feed, Cape Town) and water *ad libitum* (n= 10). HFD fed group received HFD and water *ad libitum* (n= 10). CFD fed group received HFD and 15% sucrose/fructose in drinking water *ad libitum* (n= 10). Diets were administered for twelve months.

2.4 Food intake

Food intakes were measured during the last month before termination and expressed as amount of calories consumed. Calories of 15% sucrose/fructose solution: (15/100) x 4 kcal/g)) = 0.6 kcal/g of energy (Stanfield and Hui, 2009).

2.5 Body weights and retroperitoneal fat (RF) weights

Body weights were recorded at termination of the studies. RF pads (Fig 5) were excised from the rats and weighed as a measurement of adiposity and to estimate the degree of obesity.

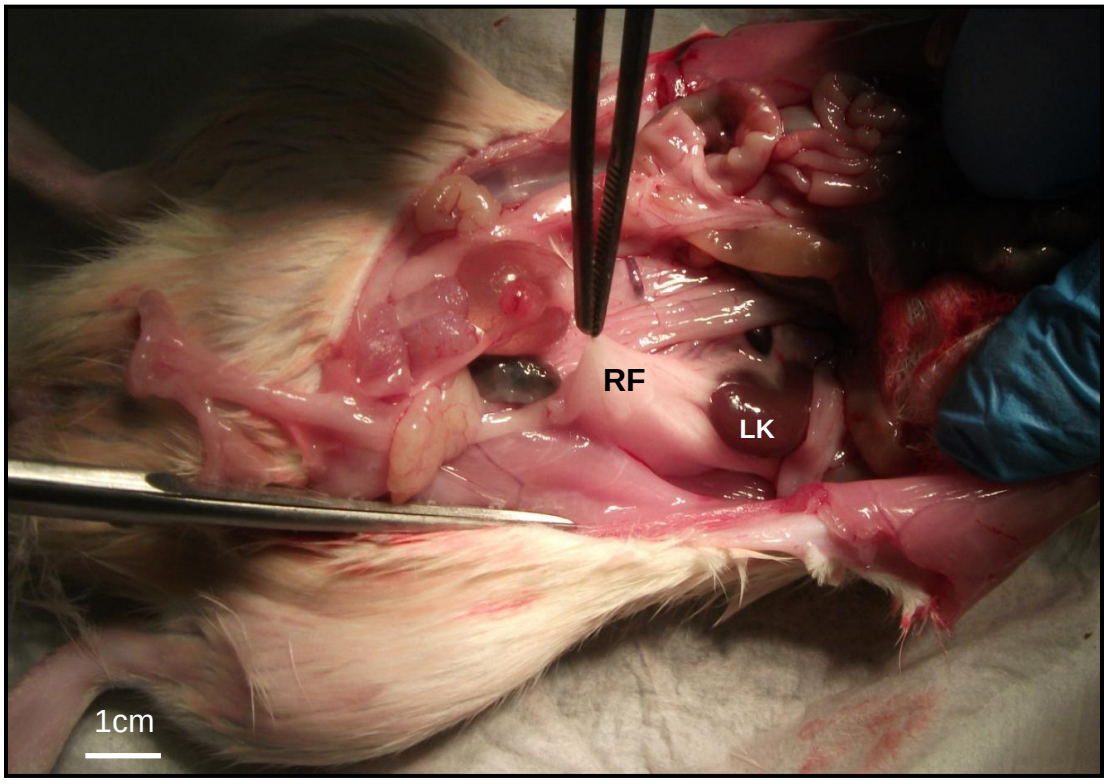

Figure 5: Photograph presentation of left RF pad with the left kidney (LK) attached

2.6 Intravenous Glucose Tolerance Test (IVGTT) and glucose stimulated insulin secretion rate (GS-ISR) combined with radioactive labeled glucose

Baseline blood samples were collected from tip of the tail prior to intravenous glucose administration. For the IVGTT and GS-ISR five rats from each group were anaesthetized by inhalation of 98% oxygen and 2% fluothane (AstraZeneca Pharmaceuticals). Once anaesthetized, a cannula (26 gauge, Neotec Medical Industries, Singapore) was inserted into the tail vein and 500 microliters (µl) prewarmed radioactive labeled 2-deoxy-[^{3}H]-D-glucose (53Ci/mmol specific activity, Amersham Bioscience) solution at a dose of 1µCi/500g in 1 milliliter (ml) sterile saline was injected intravenously over 1 minute (min) to determine intramuscular, liver and fat glucose uptake. Followed by 500 mg/kg of 50% prewarmed (35°C) dextrose (Dextrose-Fresenius 50%, PE, SA) for the measurement of intravenous glucose tolerance and glucose stimulated insulin secretion. Following administration of 2-deoxy-[^{3}H]-D-glucose and dextrose, plasma glucose concentrations were measured after 1, 2, 3, 5, 10, 20, 30, 40, 50 and 60 min. Five hundred µl blood samples, for insulin determination (refer to section 2.8), were collected at 5, 10, 30 and 60 min and samples stored in -20°C until analyzed. After one hour the rats were euthanized with 50 mg/kg sodium pentobarbital euthanase (Bayer Pty.Ltd., Animal Health Division, Isando, SA) via intraperitoneal injection. Abdominal fat, skeletal muscle and liver tissue was harvested in cryotubes and snap frozen in liquid nitrogen. Samples were stored in -80°C until analyzed as described in section 2.15.

2.7 Blood collection and organ harvesting

After three and twelve months on their respective diets, the remaining five rats per group were starved for three hours before blood collection and sacrifice. Fasting blood glucose concentrations were measured from the tail tip using a glucometer (Asencia, Bayer

Healthcare, Mishwaka, USA). Rats were anesthetized by sodium pentobarbital intra-peritoneal injection and blood was collected in Vacutainer® SST™ (BD Biosciences, Woodmead, SA) gel tubes from the abdominal vena cava. After collection, blood was centrifuged at 4000 rpm for 15 min at 4°C and serum was removed and stored at -20°C for insulin determination (refer to section 2.8). After blood collection the rats were euthanized by exsanguination under anesthesia. The pancreas, liver, kidney, heart and muscle were removed and fixed for histological evaluation in 10% phosphate buffered formalin overnight. A sample of pancreas was also placed in 2.5% glutaraldehyde (Merck, Darmstadt, Germany) in 0.1M phosphate buffer pH 7.2 for electron microscopy. Only pancreas sections were used in this study.

2.8 Insulin determination

Serum insulin concentrations were determined by radioimmunoassay (RIA) using a Linco rat insulin kit (Linco Research, St. Charles, MO, USA). Procedure was done over two days.

On the first day, standards and quality controls were prepared according to manufacturer's instructions and samples were prepared in duplicate. Two hundred µl assay buffer was added to borosilicate tubes followed by 100 µl of the rat serum samples. One hundred µl of ^{125}I-Insulin was then added to samples. One hundred µl of rat insulin antibody was then added to all the samples. Samples were then vortexed, covered and incubated overnight at 4°C.

The following day, a volume of 1 ml precipitating reagent was added to all samples. Samples were then vortexed and incubated for 20 min at 4°C. Samples were centrifuged at 4°C for 30 min at 4000 x g. The supernatant were aspirated and the visible pellet remained in tube.

Samples were analyzed using a gamma counter (Perkin-Elmer precisely wizard 1470 automatic gamma counter, Monza, Italy). Results were expressed in ng/ml.

2.9 Calculation of Homeostatic model assessment of insulin resistance (HOMA-IR)

(Method adapted from Shinohara *et al*, 2002)

HOMA-IR was used to estimate the degree of insulin resistance (Bonora *et al*, 2002; Shinohara et al, 2002). HOMA-IR was computed using the fasting plasma glucose concentrations (fPG) (mmol/l) multiplied by the fasting serum insulin concentrations (fINS) (ng/ml) divided by 22.5 ((fPG x fINS) / 22.5). A low HOMA-IR value indicates high insulin sensitivity and a high HOMA-IR indicates low insulin sensitivity (insulin resistance) (Bonora *et al*, 2002).

2.10 Calculation of glucose clearance rate (GCR)

Glucose clearance rate was calculated using the formula: (0.693 / (t-10)) x 100 as described by Kanter *et al* 1988.

2.11 Calculation of AUC

Area under the curve values were calculated using the trapezoidal method (Graphpad Prism version 5.02, Graphpad).

2.12 Preparation of tissues for histology

Tissue samples were fixed in buffered formalin (pH 7.4) for 12 hours, labeled with the

appropriate histology number and placed in tissue cassettes. The cassettes were then placed in an automated histology tissue processor (Leica TP 1020, Leica Microsystems, Nussloch, Germany) and processed overnight according to a set program (Table 2).

Table 2: Processing schedule for tissue

Carousel position	Reagent	Time (hours)
1	10 % formalin	12 hour fixation
2	70% alcohol	1
3	80% alcohol	1
4	95% alcohol	2
5	95% alcohol	1
6	100% alcohol	2
7	100% alcohol	2
8	Xylene	1
9	Xylene	1
10	Xylene	1
11	Wax	2
12	Wax	3

The total running time for a complete cycle was 17 hours.

2.12.1 Tissue imbedding and sectioning

The tissue cassettes were removed from the processor and embedded in paraffin wax. Sections, ranging between 5 - 7 µm in thickness, were then cut using a rotary microtome (Leica RM 2125 RM, Leica Microsystems, Nussloch, Germany) floated onto warm (30°C) water to remove wrinkles and placed onto 3-aminopropyltriethoxy-Silane (APES) coated slides.

2.12.2 Coating of APES slides

Sections were placed in metal slide staining racks and immersed in acetone for 2 min to remove any dirt from the slides. Sections were air dried for 5 min. Two % APES solution were prepared in acetone (98 ml acetone + 2ml APES). Sections were immersed in 2% APES solution for 2 min. Sections were washed in acetone by dipping sections approximately 10 times and this step was repeated twice. Sectioned were allowed to dry at 60°C in an incubator for approximately 30 min.

2.13 Immunohistochemistry (IHC)

Alpha (α) and β-cells were identified by immunostaining using anti-insulin (monoclonal mouse anti-insulin, clone K36aC10, Sigma Immunochemicals, St. Louis, MO, USA) and anti-glucagon antibodies (polyclonal rabbit anti- glucagon, Dako Cytomation, Carpinteria, CA, USA). Immunohistological staining to demonstrate cell proliferation was performed using MIB 5 (monoclonal mouse anti-rat Ki-67 antigen, clone MIB5, Dako, Glostrup, Denmark) and insulin (Polyclonal guinea pig anti-insulin, Dako, Carpinteria, CA, USA) antibodies. The effect of the diets on glucose transport was assessed by IHC staining of GLUT2 (WAK-Chemie, Bad Soden, Germany).

2.13.1. Double immunolabeling for glucagon and insulin in the rat pancreas

(Method adapted from Cerf *et al*, 2005).

Procedure was performed over two days.

On the first day sections were dewaxed in an oven at 60°C for 30 min, placed in xylene for 20min, hydrated in 95% ethanol for 4 min and rinsed in water. The sections were then

incubated for 5 min in 3% hydrogen peroxide (H_2O_2) to block for endogenous peroxidases. The sections were rinsed in 50 mM-tri(hydroxymethyl)-aminomethane (Tris) buffered saline (TBS) for 5 min in a staining jar on a magnetic stirrer at pH 7.2. To block non-specific binding sections were incubated for 20 min in 1:20 normal goat serum (NGS) (MRC Animal facility, Delft, SA). This prevents the secondary antibody from cross-reacting with endogenous immunoglobulins in the tissue and eliminates non-specific fragment crystallizable region (Fc region) binding of both the primary and secondary antibody. After blotting the excess serum, a 1:50 dilution of the primary antibody, anti-glucagon, was added, and the sections were incubated for 30 min at room temperature. Thereafter, the sections were jet washed with TBS and rinsed in TBS for 5 min. After rinsing, sections were incubated in a dilution of 1:1000 biotinylated anti-rabbit IgG (Vector laboratories, Burlingame, CA, USA) for 30 min in a moisture chamber. To remove unbound antibody sections were jet washed and rinsed in TBS buffer for 10 min. A volume of 5 ml of TBS**,** at pH 7.2, with 1 drop (20 µl) of solution A and 1 drop (20 µl) of solution B of Vectastain (Vector laboratories, Burlingame, CA, USA) was applied to the sections and incubated for 60 min at room temperature. Sections were then washed in TBS buffer for 10 min at pH 7.2. Immunostaining was visualized using liquid diaminobenzidine tetrachloride (DAB) Plus Substrate Chromagen System (Dako Corporation, Carpinteria, CA, USA) using 1 drop (20 µl) DAB chromagen per 1 ml of substrate buffer provided. An insoluble brown reaction DAB precipitate developed at the glucagon antibody/antigen binding site. Before applying the second primary antibody, sections were washed and rinsed with distilled water for 5 min. After rinsing and drying the slides, 1:20 normal horse serum (NHS) (MRC Animal facility, Delft, SA) was applied to slides in a moisture chamber and incubated for 20 min at room temperature. Excess serum was blotted and a dilution of 1:10000 anti-insulin (Sigma Immunochemicals St. Louis, MO, USA) was applied to sections in a moisture chamber and incubated overnight (16 hours) at 4°C.

Following overnight incubation, sections were jet washed and rinsed with 0.05M TBS for 5 min. One hundred µl of rabbit/mouse link (Envision G/2 System/AP, Rabbit/Mouse Kit, Dako, Denmark) were then added to slides and incubated for 30 mins. After incubation and washing in TBS for 10 min, AP Enzyme Enhancer (Envision G/2 System/AP, Rabbit/Mouse Kit, Dako, Denmark) was applied to sections and incubated in a moisture chamber for 30 min at room temperature. Sections were washed with 0.5M TBS. One hundred µl of substrate working solution (Envision G/2 System/AP, Rabbit/Mouse Kit) was applied to each section for 3 min. An insoluble red reaction of the permanent red precipitate developed at the insulin antibody/antigen binding site. Sections were washed and rinsed with distilled water for 5 min before counterstaining with Mayers Haemotoxylin for 2 min. Sections were then left to "blue" in running tap water for 30 min and blotted on paper towel to remove water. After air drying, the sections were mounted with Entellan® (Merck, Darmstadt, Germany) and cover slipped.

To verify the specificity of the immunohistochemistry, three negative method controls were included with each batch of sections stained. To demonstrate non-specific binding of link antibodies and endogenous enzyme activity both the primary antibodies (glucagon and insulin) were omitted. A second method control was included where the insulin antibody was omitted thereby demonstrating the specificity of glucagon staining. A third method control was included where the glucagon antibody was omitted thereby demonstrating the specificity of insulin staining.

2.13.2 Immunolabeling for GLUT2

(Method adapted from Cerf *et al*, 2006)

Sections were dewaxed as described at the beginning of section 2.13.1. The hydrated sections were then incubated in 3% H_2O_2 in distilled water for 5 min to inhibit tissue endogenous peroxidases. After exposing the slides to the H_2O_2, the sections were washed in TBS for 10 min. To reduce non-specific antibody binding the sections were incubated in 1:20 diluted NGS for 20 min. Excess serum was blotted and the primary rabbit anti-rat GLUT2 (WAK-Chemie, Bad Soden, Germany) antibody diluted 1:300 was applied to the sections for 30 min. After incubation the sections were washed in TBS for 5 min and rabbit biotinylated antibody was added for 30 min, followed by another 5 min wash in TBS. The sections were then incubated in avidin D-biotinylated horseradish H complex (Vectastain) for 60 min. Immunolabeling was revealed by incubating the sections for 5 min in liquid DAB Plus Substrate Chromagen System (Dako Corporation, Carpinteria, CA, USA). GLUT2 antibody/antigen binding was visualized by the brown DAB precipitate. The sections were counterstained with haematoxylin for 2 min, mounted with Entellan® and cover slipped.

To verify the specificity of GLUT2 staining method controls were included, where the primary antibody (GLUT2) was omitted.

2.13.3 Double immunolabelling for MIB5 and insulin in the rat pancreas

Sections were labeled over two days.

Sections were dewaxed as described at the beginning of section 2.13.1. The sections were then incubated in 3% H_2O_2 in distilled water for 5 min to inhibit tissue endogenous peroxidases. Antigen retrieval was performed in 0.01 M citrate buffer pH 6.0 at 125°C for 30

seconds and 90°C for 10 seconds using a Pascal pressure cooker (Dako Cytomation, CA, USA). Sections were then removed from Pascal and allowed to cool for 20 min. Sections were rinsed with TBS for 5 min. After rinsing and drying the slides, 1:20 NHS was applied to slides in a moisture chamber and incubated for 20 min at room temperature. After blotting the excess serum, a 1:50 dilution of the primary antibody, anti-MIB5, was added, and the sections were incubated in moisture chamber overnight (16 hours) at 4°C.

After overnight incubation insulin labeling was performed as described previously for insulin and glucagon double-immuno labeling (Section 2.13.1 Day 2). The difference being the insulin antibody used was a polyclonal guinea pig anti-insulin (Dako, Carpinteria, CA, USA).

To verify the specificity of the IHC staining, three negative method controls were included with each batch of sections stained. To demonstrate non-specific binding of the relevant link antibodies and endogenous enzyme activity both the primary antibodies (MIB5 and insulin) were omitted. A second method control was included where the MIB5 antibody was omitted thereby confirming the specificity of the link antibody binding and enzymatic detection of insulin. A third method control was included where the insulin antibody was omitted thereby demonstrating the specificity of the MIB5 immunostaining. Positive MIB5 controls were included using gastrointestinal tract sections as the mucosa have high rates of proliferation.

2.14 Electron microscopy imaging and staining

(Method: Diagnostic Electron Microscopy Unit, Anatomical Pathology, NHLS, Tygerberg Hospital, Tygerberg)

2.14.1 Tissue preparation

Pancreas tissue was fixed in 2.5% glutaraldehyde (Merck, Darmstadt, Germany) in 0.1M phosphate buffer pH 7.2 at 4°C for overnight for 16 hours. The fixed pancreas tissue was cut into 1mm blocks for processing. After a 5 min wash in phosphate buffer the tissue was fixed in 3% osmium tetroxide (Merck, Darmstadt, Germany) in Palade's buffer (2.89 g sodium barbitol (Merck, Darmstadt, Germany) and 1.15 g sodium acetate (Merck, Darmstadt, Germany) in 100 ml distilled water) for 1 hour. After the secondary fixation in osmium tetroxide the tissue was washed in distilled water and transferred into processing baskets and processed with a Leica EM Tissue Processor (Leica Microsystems, Nussloch, Germany) according to an established protocol (Table 3).

Table 3: Tissue processing schedule for electron microscopy

Carousel position	Reagent	Time (min)
1	10% uranyl acetate	15
2	70% alcohol	10
3	70% alcohol	10
4	10% uranyl nitrate	20
5	100% alcohol	15
6	100% alcohol	20
7	100% alcohol	30
8	100% alcohol : Spurr's resin	90
9	Spurr's resin	60
10	Spurr's resin	60
11	gelatine capsule	2

Tissue sections were then embedded in Spurr's resin (TAAB Laboratories Equipment Ltd., UK) into gelatine capsules (Eli Lilly, SA) overnight at 60°C. Blocks were allowed to cool and carefully marked.

2.14.2 Tissue sectioning and staining

A Leica EM UC7 (Leica Microsystems, Nussloch, Germany) ultratome was used to cut ultra thin (100 nm) sections from the resin blocks. Glass knives were made using a knifemaker (LKB 7800, Biostad, Canada) and glass strips (LKB, Biostad, Canada). A water trough was attached to each knife by using autoclave tape and melted dental wax. Ultra thin sections were collected from the water surface onto 200G mesh copper wire grids (Wirsam Scientific, SA) allowed to dry on filter paper before staining. To enhance contrast, the grids were firstly stained with 2% uranyl acetate (Agar Scientific Ltd., SA) in 70% alcohol for 10 min. Thereafter the sections were rinsed in 70% alcohol and distilled water. To further increase cell membrane contrast, the grids were stained with Reynold's lead acetate (2.66g lead nitrate (Merck, Darmstadt, Germany) and 3.52 g sodium citrate (Merck, Darmstadt, Germany) in 60 ml distilled water) for 5 min. Finally the grids were washed in distilled water, allowed to dry on filter paper and then scoped with a JOEL GEM 1011 (JOEL Ltd, Japan) transmission electron microscope.

2.15 Assays of 2-deoxy-[^{3}H]-D-glucose uptake- muscle, liver and fat tissue

(Method adapted by Chadwick et al, 2007)

Tissues collected (as described in section 2.7) were weighed and placed in Eppendorf tubes. An equal volume of 30% potassium hydroxide (KOH) in µl's, per tissue weight (i.e. 242 mg tissue + 242 µl 30% KOH) was added to the tissue in the Eppendorf tube and the tube placed in a boiling beaker of water for 5-30 min until dissolution of the tissue. Once dissolved, samples were removed from the beaker, thoroughly mixed and transferred to glass vials. In liver and fat tissue 100 µl of 30% H_2O_2 was added to bleach samples. After the initial reaction (after foaming ceases), and to complete discoloration, a second addition of 100 µl 30% H_2O_2

was added. Eight ml liquid scintillation cocktail (Ultima Gold, Perkin Elmer, CT, USA) was added to the vials and allowed to equilibrate overnight for 16 hours then counted in a scintillation counter (2200CA Tri-carb Series, Packard Instrument Company, IL, USA).

Data were expressed as counts per minute (cpm) and disintegrations per minute (dpm) values. Results were analyzed using the dpm value per gram of tissue sample (Chadwick *et al*, 2007; Verhelst *et al,* 1998). Each sample was read for 10 min. All samples were done in triplicate. Sample readings were normalized according to a standard curve for tritium [^{3}H] that is installed in the 2200CA Tri-carb Series liquid scintillation counter when calibrated.

2.16 Image analysis of immuno-labeling for glucagon and insulin

2.16.1 Image capture

Stained sections of pancreata were captured using the x10 objective attached to an Olympus BX60 light microscope equipped with a digital camera (Leica DC290, Wetzlar, Germany) and interfaced with Leica Qwin Professional software (Leica, Wetzlar, Germany). Every alternate field was scanned and saved as a tiff image with a resolution of 768 x 1024 pixels. Five slides per group were evaluated.

2.16.2 Calibration

The software was calibrated for the x10 objective using the inner squares of Neubauer cell chamber, which has a known area of 2500 μm^2. The square areas were determined by red, green, blue (RGB) colour segmentation of 1, 2, 3, 4, 8, 12 and 16 squares. The determined areas were plotted against the actual known measurements using a line graph. The slope of the line was checked for linearity.

2.16.3 Using the correct calibration

In order to use the correct calibration for a specific objective lens, the correct lens was selected in the Qwin select lens feature and the update feature was selected in the system calibration feature.

2.16.4 Image analysis

For the determination of tissue areas, each image was subjected to RGB colour segmentation so that the whole section surface was selected and converted to a binary image. The area of the binary image was determined and the data automatically transferred to Microsoft Excel. To determine islet areas, images containing islets were subjected to RGB colour discrimination to select both the insulin positive (red) and glucagon positive (brown) cells. The resultant binary image was subjected to a closing function for 30 cycles and converted to a new binary image representing the whole islet, including areas not stained positively for glucagon and insulin. The area was then determined and automatically transferred to Microsoft Excel. The α-cell area was determined by subjecting the image to RGB segmentation to obtain a binary image from the glucagon positive cells (brown). The area of the binary image was determined and automatically transferred to Microsoft excel. The β-cell area was determined as for α-cell area, except that a binary image was obtained to represent the area of insulin positive cells (red).

2.16.5 Morphometrical parameters

2.16.5.1 Ratio of endocrine tissue to total tissue area

To determine ratio of endocrine to total tissue area, the total islet area was divided by the total tissue area.

2.16.5.2 Ratio of β-cell to α-cell area

β-cell area to α-cell area was determined by dividing the total β-cell area by the total α-cell area.

2.16.5.3 Islets per unit area

The total number of islets counted was divided by the total tissue area expressed in cm^2 to determine the number of islets per cm^2 of pancreas tissue.

2.16.5.4 The distribution of different sizes of islets to the total number and total area of islets

The total number of islets were counted and classified according to size as follows: 1-2500 μm^2; 2501-7500 μm^2; 7501-12500 μm^2; 12501-20000 μm^2 and >20001 μm^2. To determine the percentage contribution of the number of islets in each classification of islet size, the number of islets in each group was expressed as a percentage of the total number of islets counted. To determine the percentage contribution of the area of islets in each classification of islet size, the total area of islets in each group was expressed as percentage of the total area of islets measured.

2.17 GLUT2 immunohistochemical evaluation

Pancreatic sections stained for GLUT2 were evaluated using a light microscope at a magnification of x 100. GLUT2 positivity was assessed using an adapted scoring method as described by Kramer *et al,* 2009. The scoring method was based on the number of GLUT2 positive cells within pancreatic islets (Table 4). All sections were independently evaluated by two experienced individuals who were blinded. Five slides per group were evaluated.

Table 4: Evaluation of GLUT2 positivity

GLUT2 Scoring	
0	no visible staining in islets
1	few/scattered positive staining cells in islets
2	moderate staining of most cells in islets
3	strong staining of most cells in islets

2.18 MIB5 and insulin immunohistochemical evaluation

Pancreatic sections double labeled for MIB5 and insulin were assessed using a light microscope at a magnification of x 100. Positivity was assessed using an adapted scoring method as described by Jorda *et al* 2003 (Table 5). All sections were independently evaluated by two experienced individuals were blinded. Five slides per group were evaluated.

Table 5: Evaluation of MIB5 positivity

MIB5 Scoring	
0	no positivity
1	< 5% of β-cells staining positively
2	5% -25% of β-cells staining positively
3	>25% of β-cells staining positively

2.19 Statistical analysis

Data generated were entered into Microsoft Excel and analyzed by calculating the means and standard deviation. Statistical significance was calculated with Student's t-test or one-way ANOVA (with Dunnett's post-hoc test if $p<0.05$). A p-value of $p \leq 0.05$ was deemed to be statistically significant.

CHAPTER THREE

RESULTS

3.1 Food intake

The rats were maintained on laboratory chow diets for three weeks where after they were randomly allocated to the three different diets and maintained for either three or twelve months. The average daily calorific intake at three months of the HFD and CFD fed rats was significantly higher than the calories consumed by the control diet rats (99.94 ± 20.29 and 99.44 ± 9.21 vs. 70.53 ± 7.58 kcal/day respectively; $p<0.0001$) (Table 6 and Fig 6).

Calorific intake at twelve months of the HFD and CFD was significantly increased compared to the control (125.66 ± 13.95; $p<0.0001$ and 104.69 ± 17.42; $p=0.001$ vs. 92.56 ± 9.00 kcal/day respectively). Of interest was that the calorific intake of the rats fed a HFD was significantly increased compared to the CFD at twelve months ($p =0.02$) (Table 6 and Fig 7).

Table 6: Food and calorific intakes of different diets at three and twelve months

		Food intake: g/day	Ave kcal/g per day
3 months	Control	27.13 ± 2.92	70.53 ± 7.58
	HFD	48.51 ± 9.85	99.94 ± 20.29
	CFD	35.51 ± 5.22	99.44 ± 9.21
12 months	Control	35.60 ± 3.46	92.56 ± 9.00
	HFD	61.00 ± 6.77	125.66 ± 13.95
	CFD	33.97 ± 9.68	104.69 ± 17.42

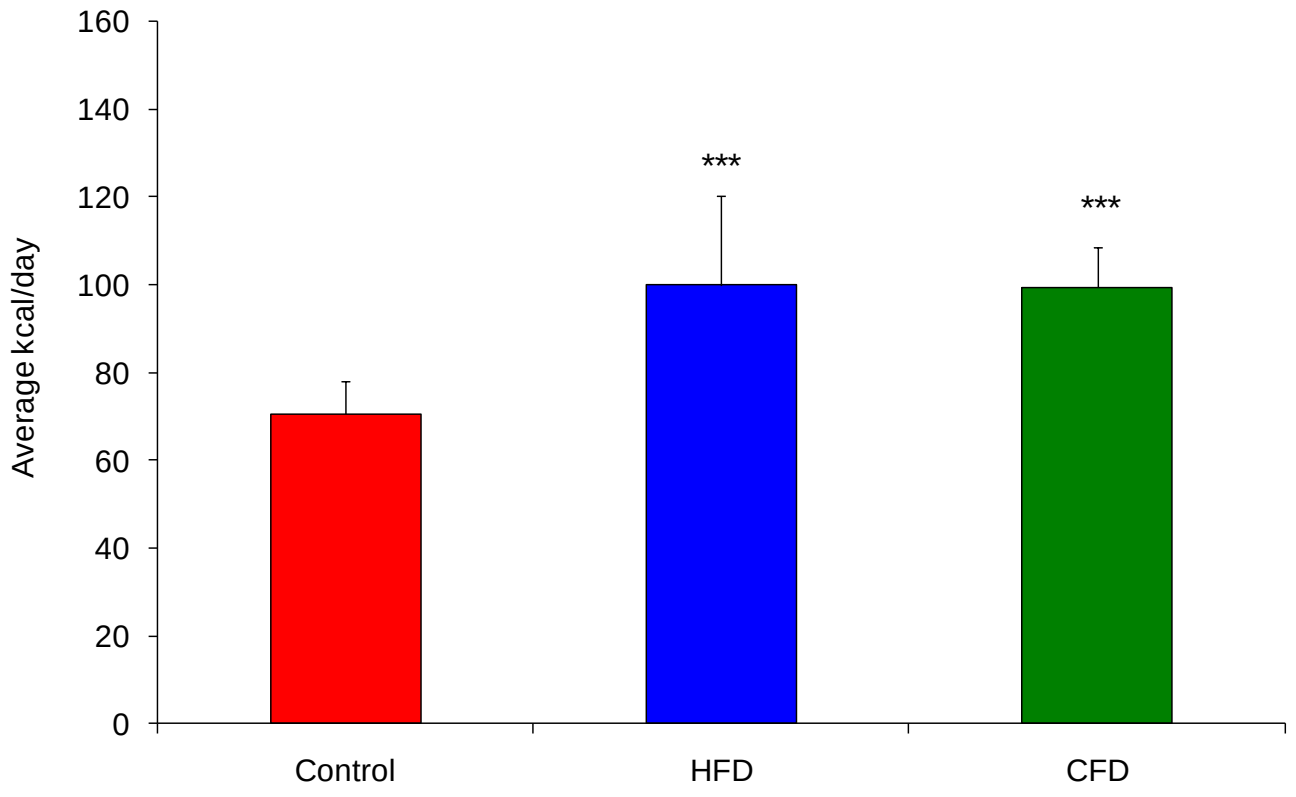

Figure 6: Calorific intake at three months

Calorie intake was calculated from food and liquid intake. Values are expressed as mean ± SD. CFD and HFD vs. control, *** $p < 0.0001$.

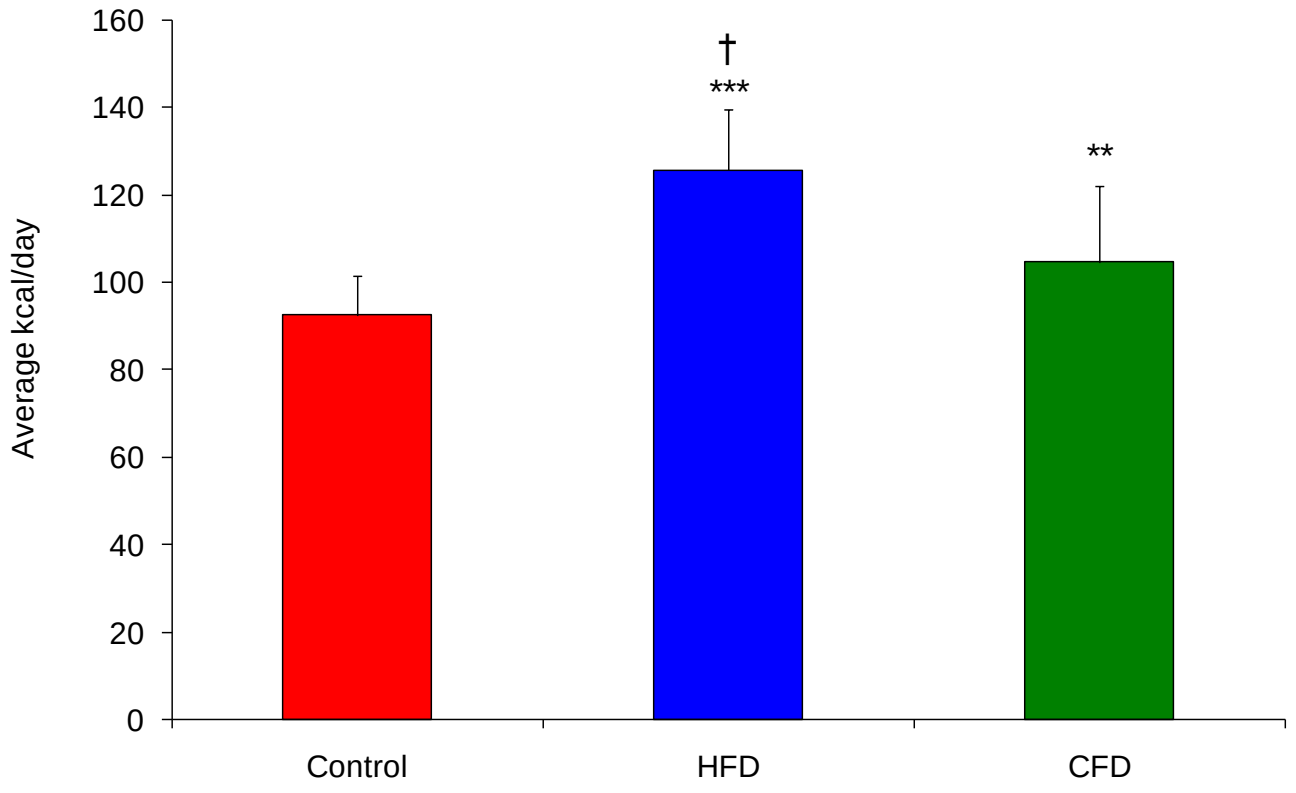

Figure 7: Calorific intake at twelve months

Calorie intake was calculated from food and liquid intake. Values are expressed as mean ± SD. CFD vs. control, ** p= 0.001; HFD vs. control, *** p< 0.0001 and HFD vs. CFD, † p= 0.02.

3.2 Body weight and retroperitoneal fat

Results shows average body weight and RF pad weight at termination of studies at three and twelve months. After three months feeding, the body mass of the rats maintained on the HFD and CFD were significantly higher compared to controls (470.90 ± 45.19 g; p=0.0147 and 528.20 ± 48.32 g; p=0.0008 vs. 394.80 ± 31.19 g) (Table 7 and Fig 8).

The RF pad weight at three months of the HFD and CFD fed rats was significantly higher than that of the control diet rats (12.35 ± 2.53 g; p=0.0001 and 18.41 ± 6.97 g; p=0.0012 vs. 3.02 ± 1.00 g) (Table 7).

After twelve months the body mass of the HFD and the CFD fed rats were significantly higher than the controls (908.61 ± 131.14 g and 947.20 ± 51.46 g vs. 599.07 ± 35.69 g; p<0.0001) (Table 7 and Fig 9). There were no significant differences in body weights between the rats fed a HFD and CFD at both three and twelve months.

The RF pad weight at twelve months of the HFD and CFD fed rats was significantly higher than that of the controls (52.72 ± 16.97 g and 56.20 ± 9.19 g vs. 10.81 ± 3.39 g; p<0.0001) (Table 7). There were no significant differences between the RF pads of rats fed a HFD and CFD at both three and twelve months.

A photograph of the HFD and control fed rat at twelve months shows the somatic changes in fat deposits between the rats fed different diets (Fig 10) and also excess fat accumulation in a rat fed HFD for twelve months (Fig 11).

Table 7: Comparison between body weight and RF weights at three and twelve months

		Body weight (g)	RF weight (g)
3 months	**Control**	394.80 ± 31.19	3.04 ± 1.00
	HFD	470.90 ± 45.19*	12.35 ± 2.53***
	CFD	528.20 ± 48.32***	18.41 ± 6.97**
12 months	**Control**	599.07 ± 35.69	10.81 ± 3.39
	HFD	908.61 ± 131.14***	52.72 ± 16.97***
	CFD	947.20 ± 51.46***	56.20 ± 9.19***

Values are expressed as mean ± SD. Body weights at 3 months: CFD vs. control, *** p=0.0008; HFD vs. control, * p=0.0147 and 12 months: CFD and HFD vs. control, *** p<0.0001. RF weight at 3 months: CFD vs. control, ** p=0.0012; HFD vs. control, *** p=0.0001 and 12 months: CFD and HFD vs. control, *** p< 0.0001.

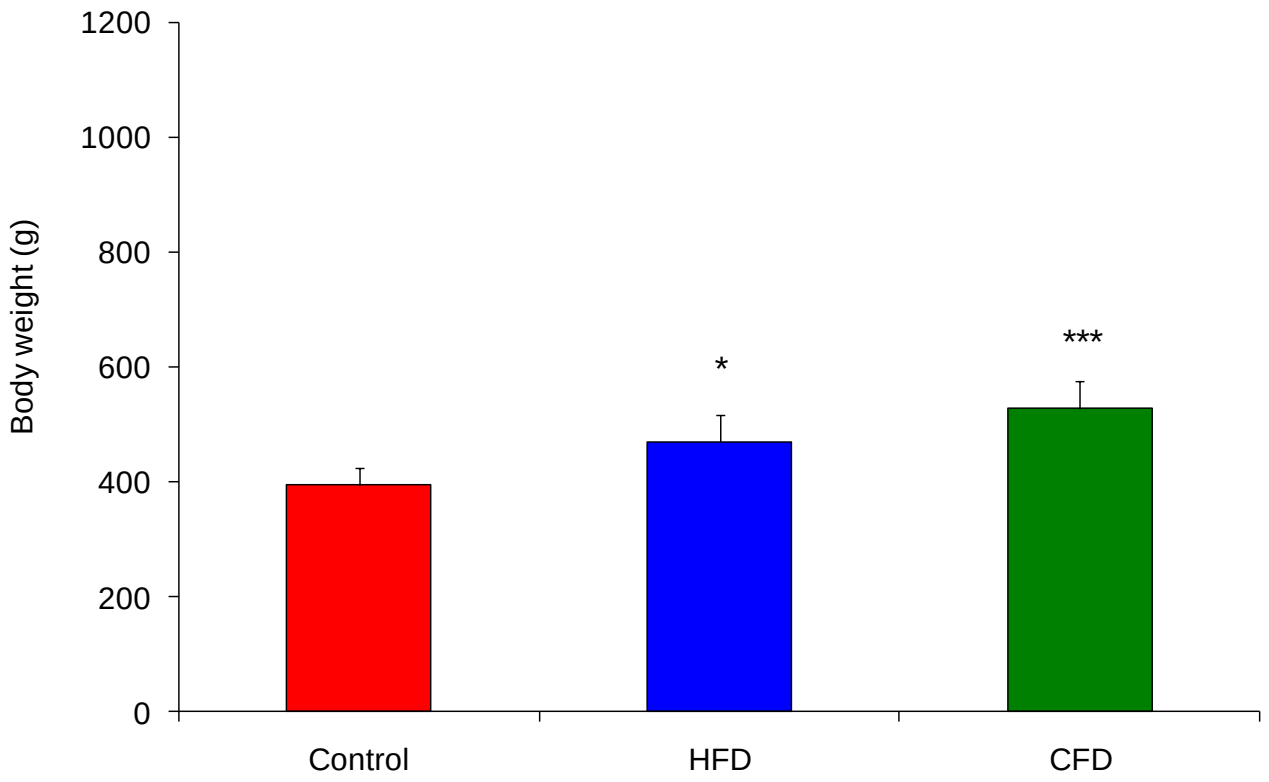

Figure 8: Body weight at three months

Values are expressed as mean ± SD. CFD vs. control, *** p=0.0008; HFD vs. control, * p=0.0147.

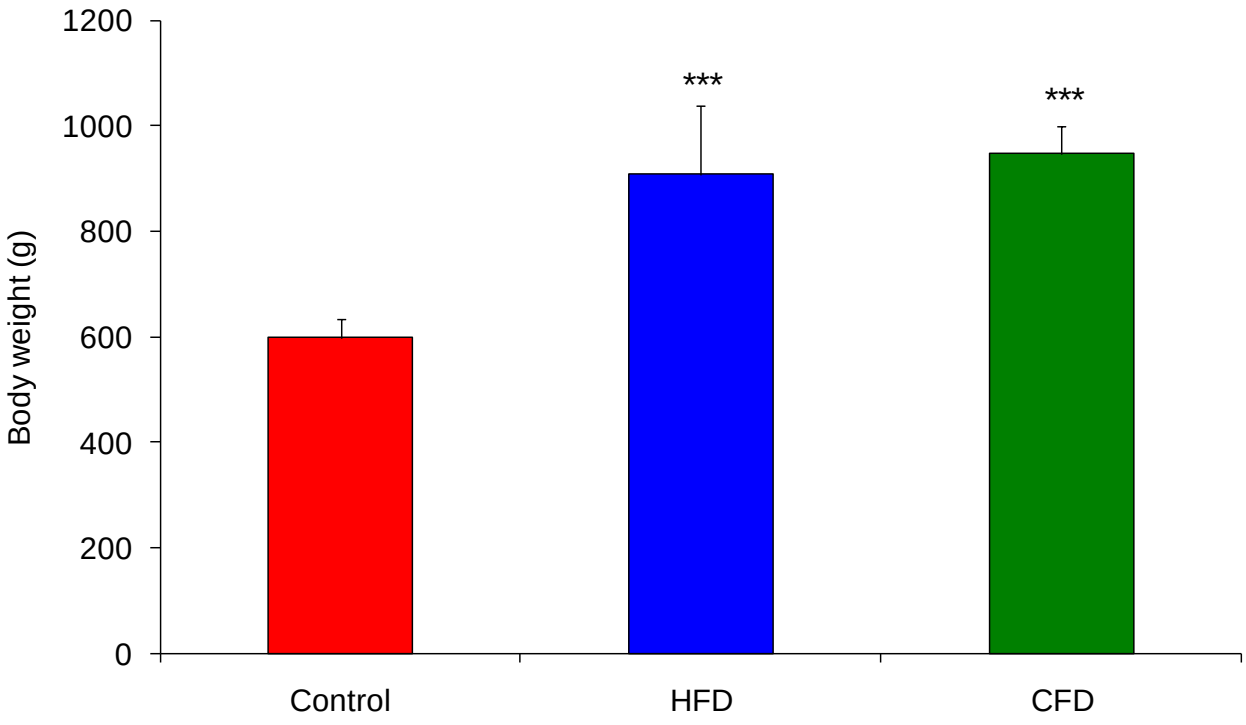

Figure 9: Body weight at twelve months

Values are expressed as mean ± SD. CFD and HFD vs. control, *** p<0.0001.

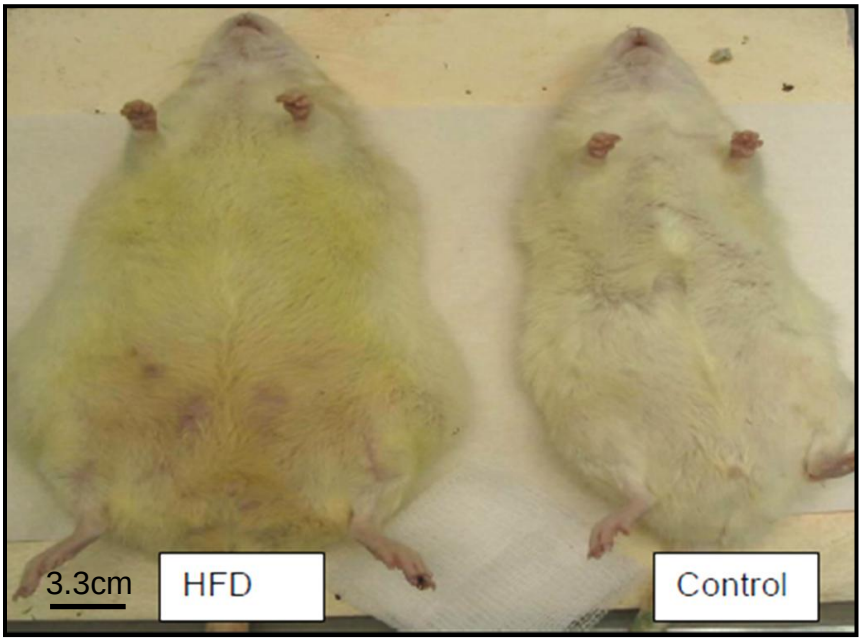

Figure 10: Photograph of Wistar rats at twelve months fed HFD and control diets

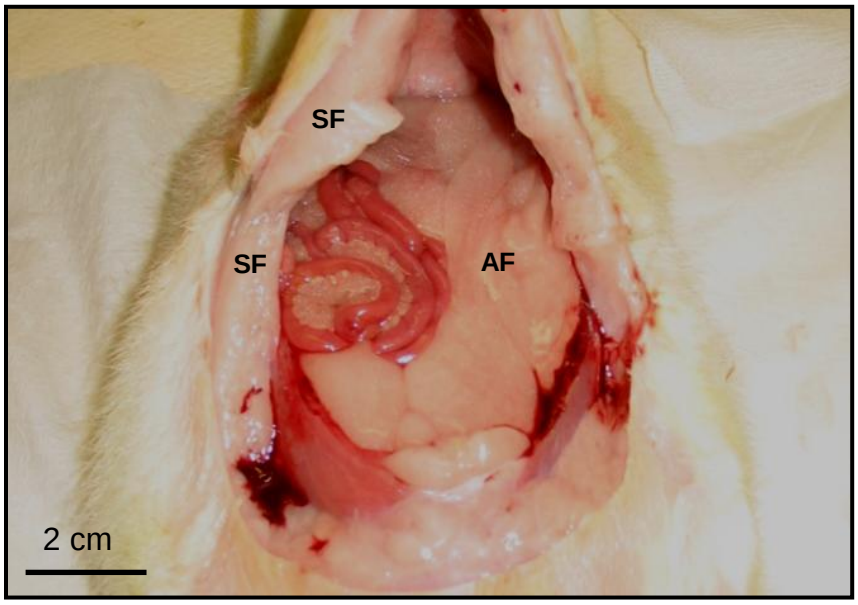

Figure 11: Photograph of Wistar rat on HFD at twelve months showing abdominal (AF) and subcutaneous fat (SF) deposition

3.3 Fasting plasma glucose and serum insulin concentrations

At three months there were no significant differences in fasting glucose concentrations between the three groups (control; 5.8 ± 10.4 mmol/l vs. HFD; 5.1 ± 11.1 mmol/l vs. CFD; 6.1 ± 0.2 mmol/l) (Fig 12). Fasting insulin concentrations showed significant increase in the CFD fed rats when compared to the control rats (15.3 ± 5.2 ng/ml vs. 6.3 ± 1.9 ng/ml; p=0.01) (Fig 12).

At twelve months fasting blood glucose concentrations were significantly increased in the CFD group compared to the control and HFD fed group (7.1 ± 1.5 mmol/l vs. 5.7 ± 0.8 mmol/l; p=0.006 and 6.1 ± 1.1 mmol/l; p=0.03 respectively) (Fig 13). In addition, fasting insulin concentrations were significantly decreased in the HFD group vs. the control and CFD fed groups (4.5 ± 2.9 ng/ml vs. 8.5 ± 5.3 ng/ml; p=0.01 and 11.6 ± 6.1 ng/ml; p=0.0003 respectively) (Fig 13).

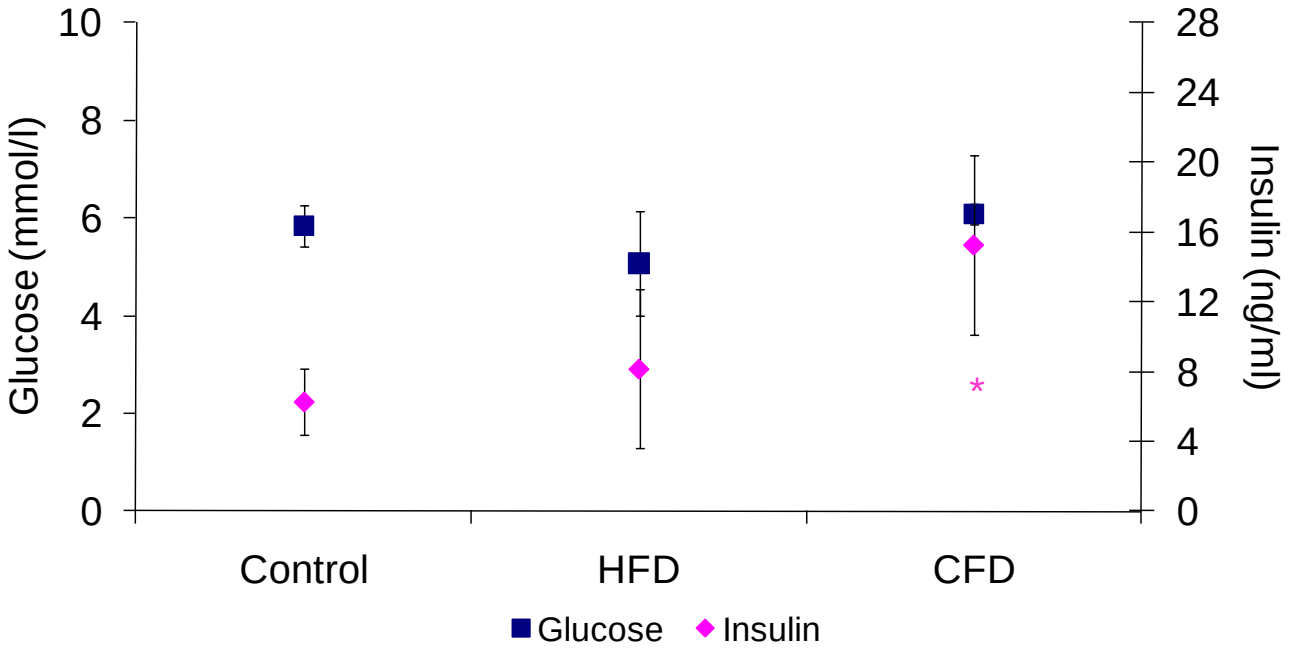

Figure 12: Fasting plasma glucose and insulin concentrations at three months

Values are expressed as mean ± SD. Glucose: $p>0.05$ in all groups compared to control. Insulin: CFD vs. control, * $p=0.01$.

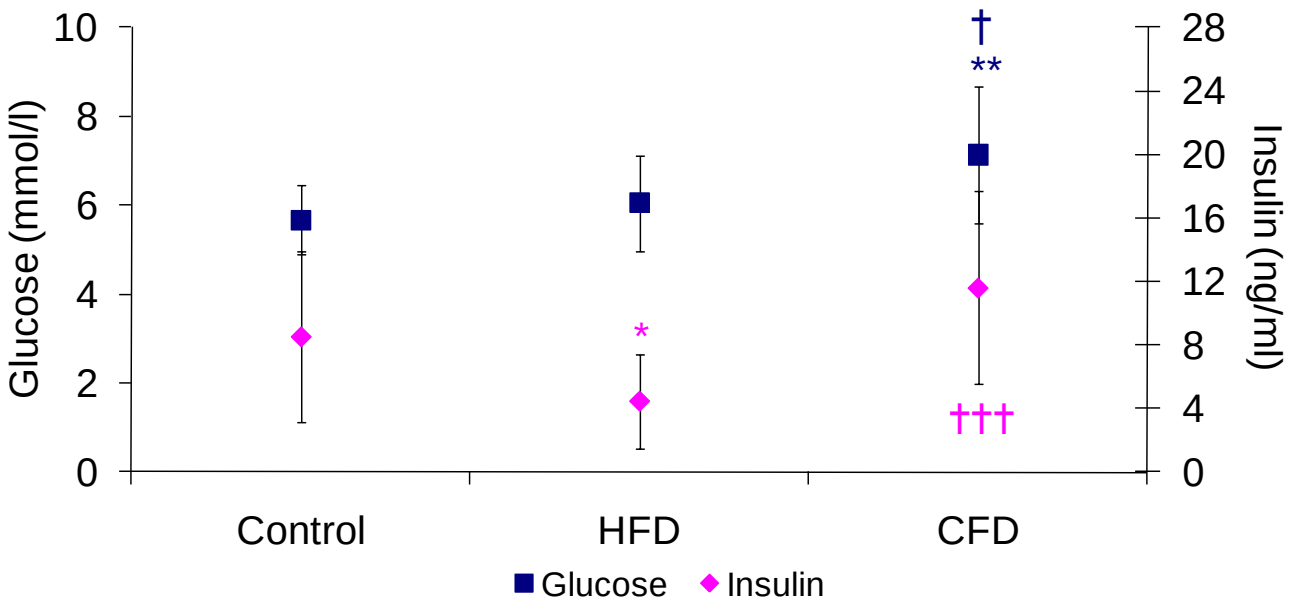

Figure 13: Fasting plasma glucose and insulin concentrations at twelve months

Values are expressed as mean ± SD. Glucose: CFD vs. controls, ** p=0.006; vs. HFD, † p=0.03. Insulin: HFD vs. control, * p=0.01; vs. CFD, ††† p= 0.0003.

3.4 HOMA-IR calculation of insulin resistance

The assessment of HOMA-IR as a degree of insulin resistance was measured using a standard formula, ((fPG x fINS) / 22.5). At three months insulin resistance as defined by HOMA-IR was significantly increased in the CFD vs. controls (4.14 ± 1.46 vs. 1.64 ± 0.55; p= 0.01) (Table 8). At 12 months HOMA-IR was significantly increased in the CFD group vs. the controls and the HFD group (3.69 ± 2.01 vs. 2.10 ± 1.31; p=0.03 and 1.28 ± 1.11; p=0.0003) (Table 8).

Table 8: Fasting glucose (fPG), insulin concentrations (fINS) and HOMA-IR values at three and twelve months

Parameters		fPG (mmol/l)	fINS (ng/ml)	HOMA-IR
3 months	Control	5.84 ± 0.43	6.28 ± 1.86	1.64 ± 0.55
	HFD	5.08 ± 1.08	8.16 ± 4.56	2.03 ± 1.19
	CFD	6.08 ± 0.20	15.27 ± 5.17*	4.14 ± 1.46*
12 months	Control	5.67 ± 0.78	8.52 ± 5.38	2.10 ± 1.31
	HFD	6.05 ± 1.07	4.45 ± 2.96*	1.28 ± 1.11
	CFD	7.14 ± 1.54**†	11.61 ± 6.07†††	3.69 ± 2.01*†

Values are expressed as mean ± SD. HOMA-IR at 3 months: CFD vs. controls, * p=0.01. At 12 months CFD vs. controls, * p=0.03; vs. HFD, ††† p= 0.0003.

3.5 Intravenous glucose tolerance test (IVGTT) and glucose stimulated-insulin secretion rate (GS-ISR)

There were no significant differences at all IVGTT time points at three months of the respective diets (Fig 14a). The AUC values also showed no difference between between groups at three months (Fig 14b). However, compared to the controls the glucose clearance rate of the HFD and CFD fed rats was diminished (3.32 ± 2.72 vs. 1.15 ± 1.10; p =0.1367 and 1.78 ± 1.07; p = 0.2739) at three months although this was not significant (Table 9). After 3 months the GS-ISR of the CFD fed group showed increased peak insulin values at 5 (6.49 ± 3.49 ng/ml) and 10 min (3.95 ± 3.34ng/ml) after glucose stimulation compared to HFD (5 min: 4.74 ± 4.69 and 10 min: 2.09 ± 2.92 ng/ml) and control (5 min: 3.58 ± 2.28 and 10 min: 1.99 ± 1.80 ng/ml) (Fig 15a). The AUC value of the GS-ISR (control: 68.60 ± 45.96; HFD: 104.80 ± 122.80; CFD: 142.20 ± 104.04; $p<0.05$) was also increased, albeit not significant (Fig 15b).

At twelve months, the IVGTT of the CFD showed increased peak values at 3 min (22.70 ± 6.28 mmol/L) compared to HFD (15.73 ± 3.23 mmol/L; p= 0.04) (Fig 16a). Glucose concentrations at 5 min (23.26 ± 2.12 mmol/L) and 10 min (19.90 ± 2.03 mmol/L) of the IVGTT were significantly increased when compared to both HFD (5 min: 15.57 ± 1.15; $p<0.0001$ and 10min: 13.60 ± 1.44 mmol/L; p= 0.0002) and controls (5 min: 14.20 ± 4.83; p= 0.003 and 10 min: 14.46 ± 4.59 mmol/L; p= 0.03) (Fig 16a). IVGTT AUC values were significantly increased in the CFD compared to the HFD and control group (850.08 ± 71.74 vs. 596.13 ± 53.05; $p<0.0001$ and 599.27 ± 131.14; p=0.003) respectively (Fig 16b). At twelve months the glucose clearance following the IVGTT bolus was reduced in all three groups (control: 1.54 ± 1.45 vs. HFD: 1.50 ± 1.33; p =0.9621 and CFD: 1.17 ± 1.11; p =0.650) (Table 9). GS-ISR at 12 months on CFD showed significantly decreased insulin secretion at

30 min (1.56 ± 1.40 ng/ml $p<0.001$) compared to HFD (5.21 ± 1.77 ng/ml) (Fig 17a). GS-ISR AUC values of the CFD (175.40 ± 113.84; $p=0.043$) were significantly decreased compared to HFD (354.67 ± 135.71) (Fig 17b).

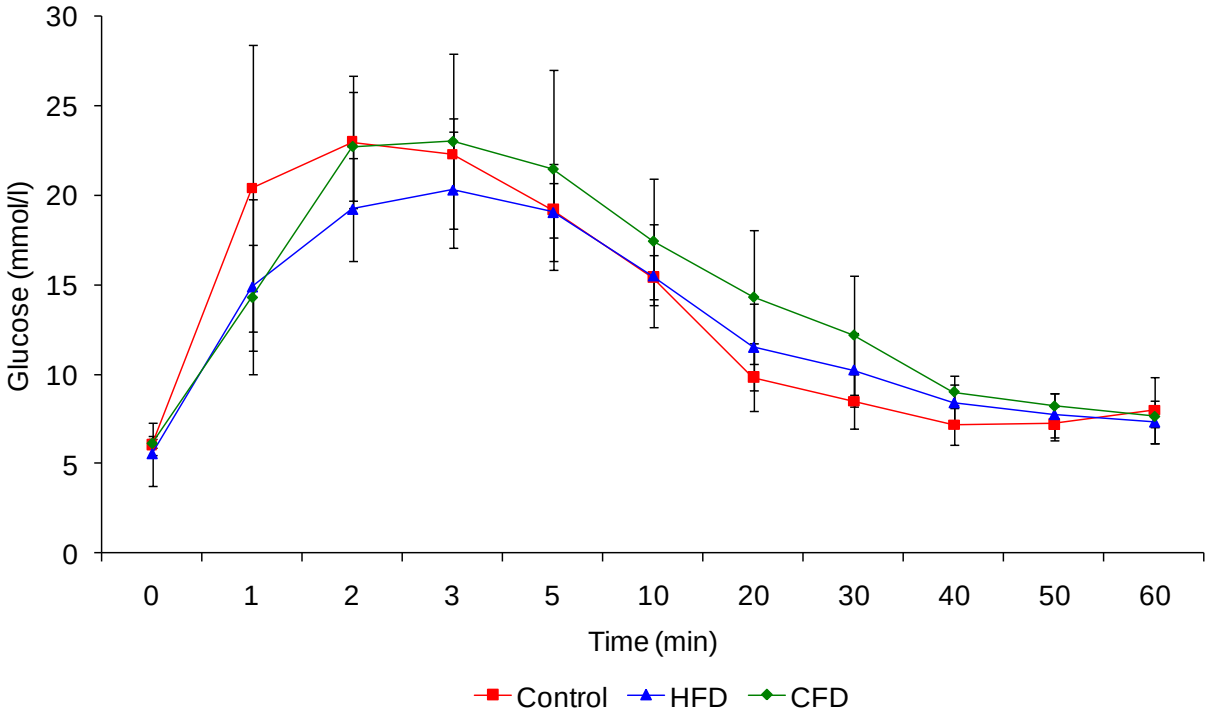

Figure 14a: IVGTT at three months

Values are expressed as mean ± SD. p>0.05 at all time points between groups.

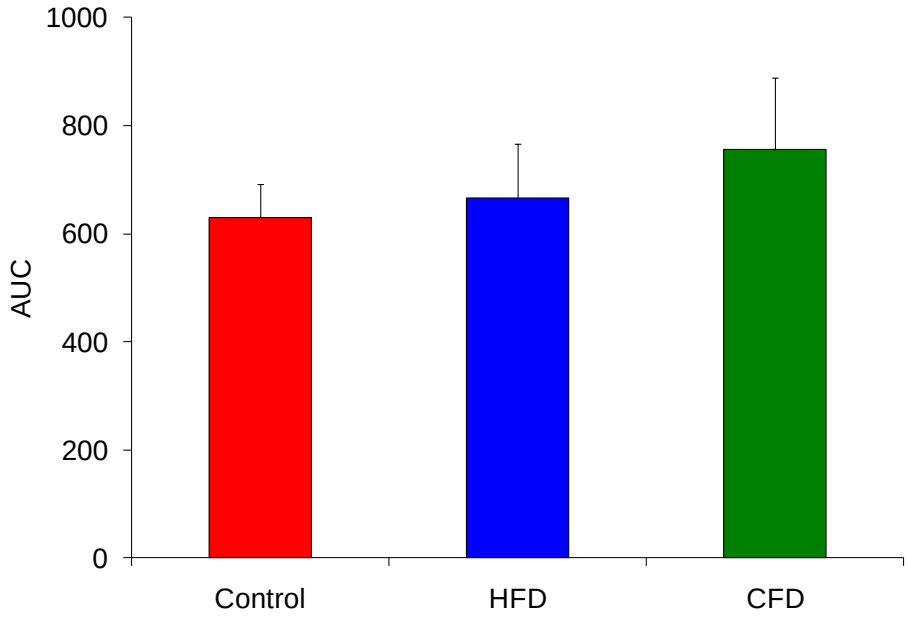

Figure 14b: AUC IVGTT at three months

Values are expressed as mean ± SD. p>0.05 at all time points between groups.

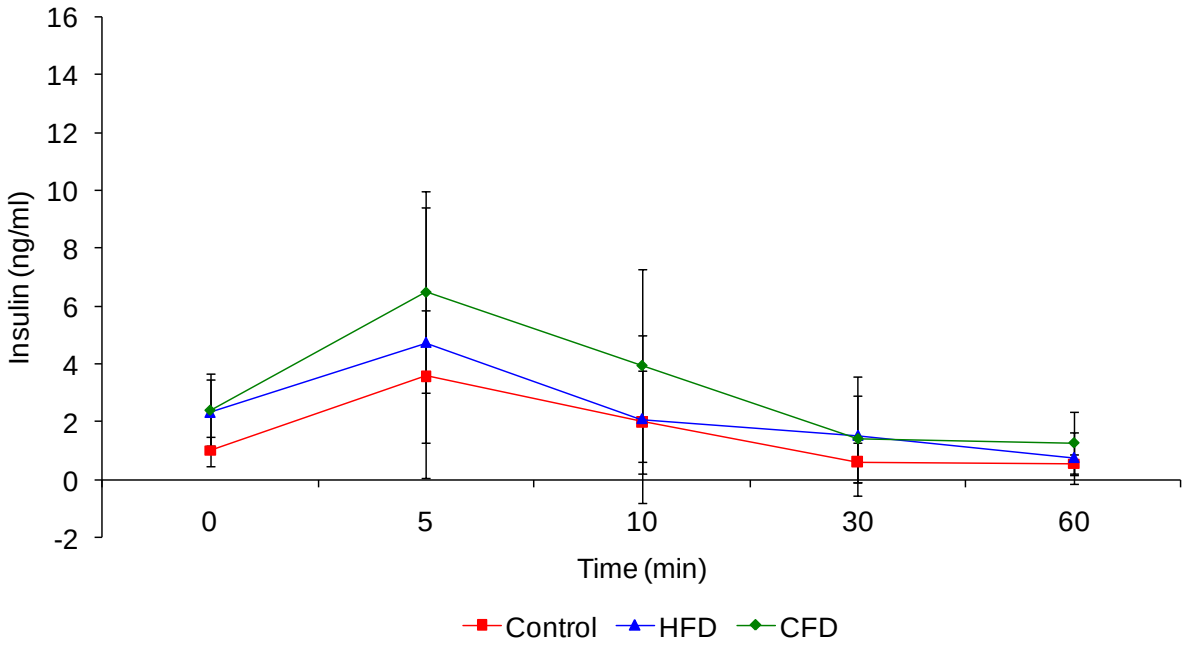

Figure 15a: GS-ISR at three months

Values are expressed as mean ± SD. p>0.05 at all time points between groups.

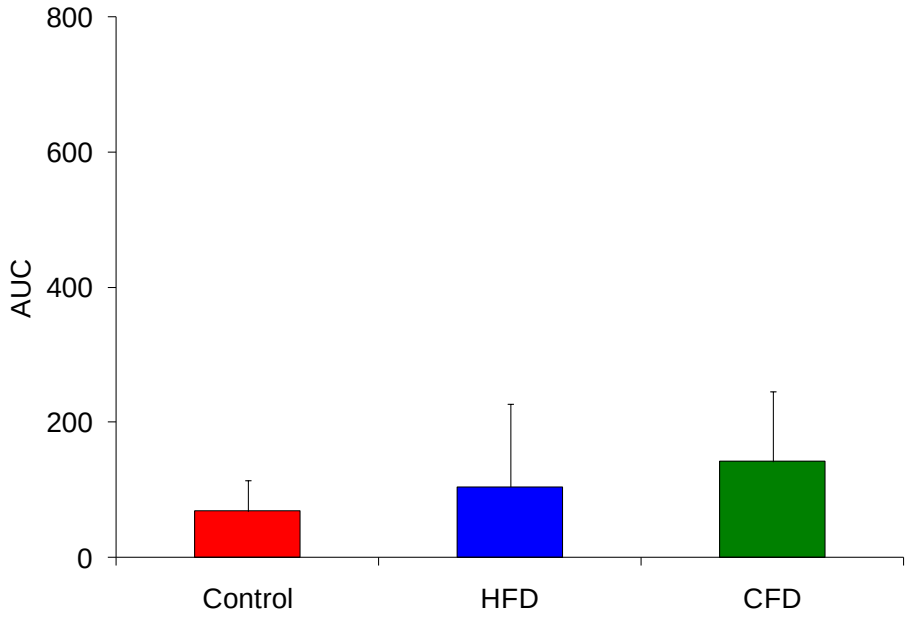

Figure 15b: AUC GS-ISR at three months

Values are expressed as mean ± SD. p>0.05 at all time points between groups.

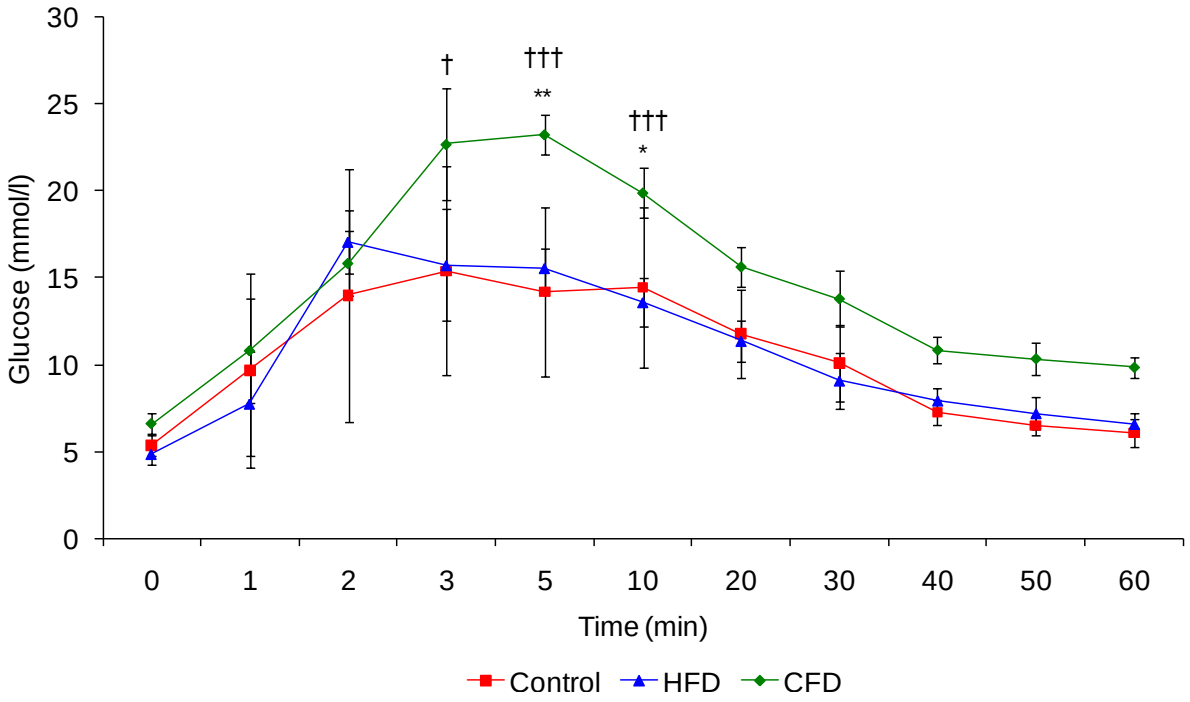

Figure 16a: IVGTT at twelve months

Values are expressed as mean ± SD. At 3 min: CFD vs. HFD, † p=0.04; at 5 min: CFD vs. HFD, ††† p<0.0001 and control ** p=0.003; at 10 min: CFD vs. HFD, ††† p=0.0002 and control * p=0.03.

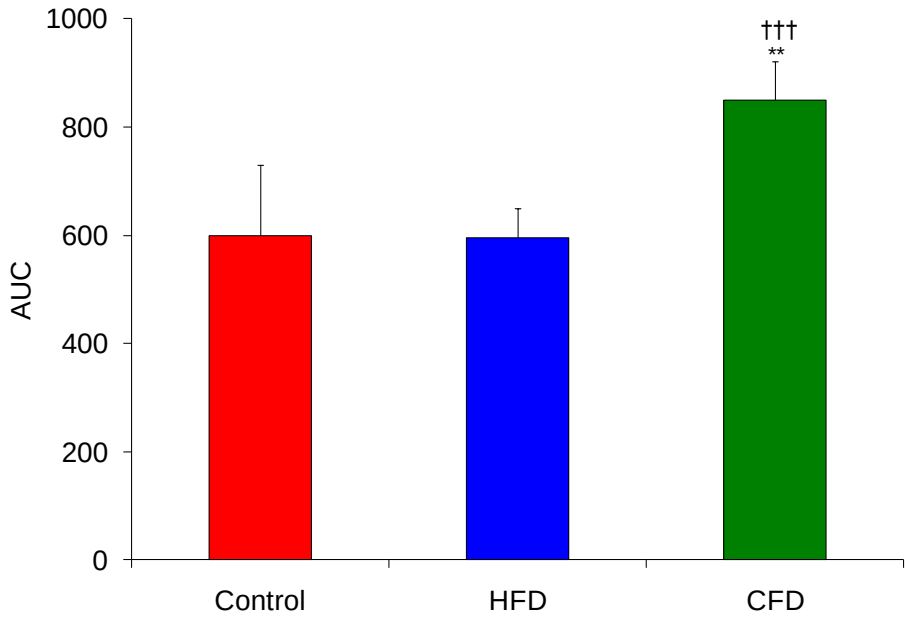

Figure 16b: AUC IVGTT at twelve months

Values are expressed as mean ± SD. CFD vs. HFD, ††† p<0.0001 and control ** p=0.003

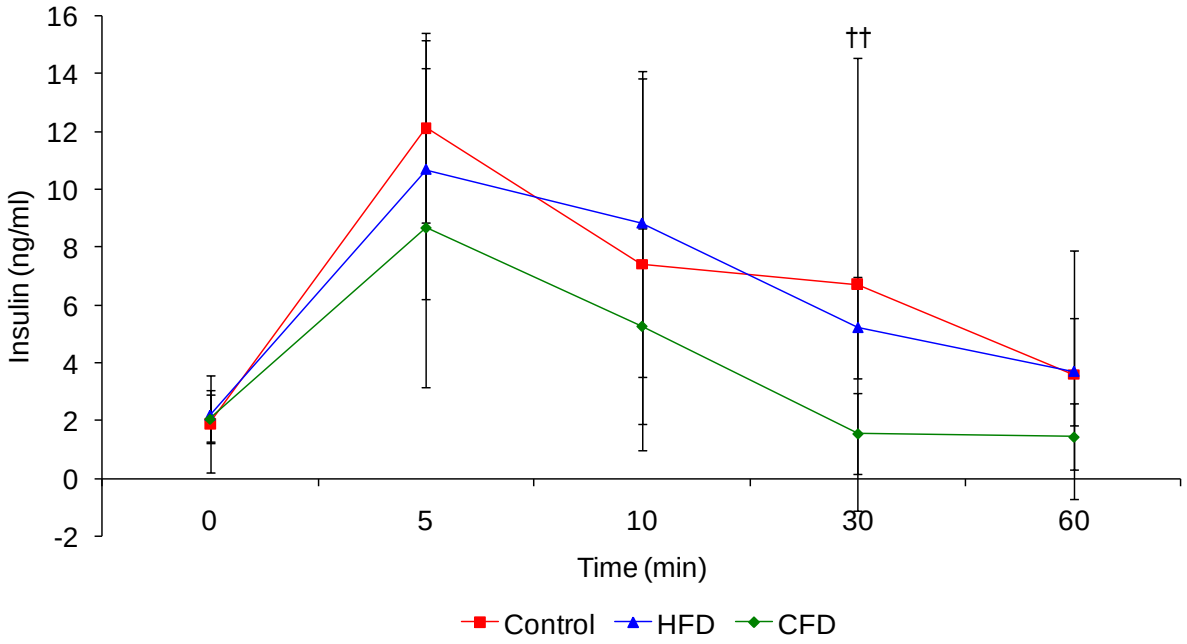

Figure 17a: GS-ISR at twelve months

Values are expressed as mean ± SD. At 30 min: CFD vs. HFD, †† p=0.0047.

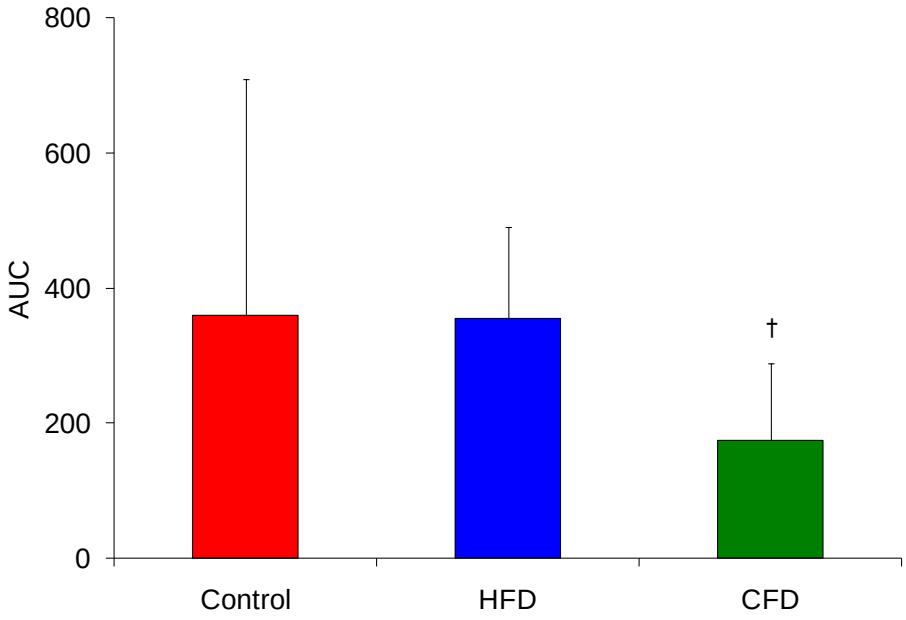

Figure 17b: AUC GS-ISR at twelve months

Values are expressed as mean ± SD. CFD vs. HFD, † p=0.043

Table 9: Glucose clearance rate at three and twelve months

Values are expressed as mean ± SD. p>0.05 in all groups compared to Control.

Glucose clearance rate		
3 months	**Control**	3.32 ± 2.72
	HFD	1.15 ± 1.10
	CFD	1.78 ± 1.07
12 months	**Control**	1.54 ± 1.45
	HFD	1.50 ± 1.33
	CFD	1.17 ± 1.11

3.6 2-deoxy-[^{3}H]-D-glucose uptake in muscle, liver and fat tissue between CFD and control rats

After three months the 2-deoxy-[^{3}H]-D-glucose uptake glucose uptake in muscle tissue of the CFD fed rats was reduced compared to the controls (17821.27 ± 2682.65 vs. 26936.87 ± 9033.56 dpm / g tissue; p=0.0008) (Fig 18). Liver glucose uptake was similar between the two groups while the uptake in adipose tissue in the CFD group was reduced compared to controls (controls: 1386.37 ± 175.15 vs. CFD: 964.18 ± 120.00; p< 0.0001) (Fig 18).

There were no significant differences in the 2-deoxy-[^{3}H]-D-glucose uptake of muscle, liver or fat tissue between controls and CFD fed rats at twelve months (Fig 19).

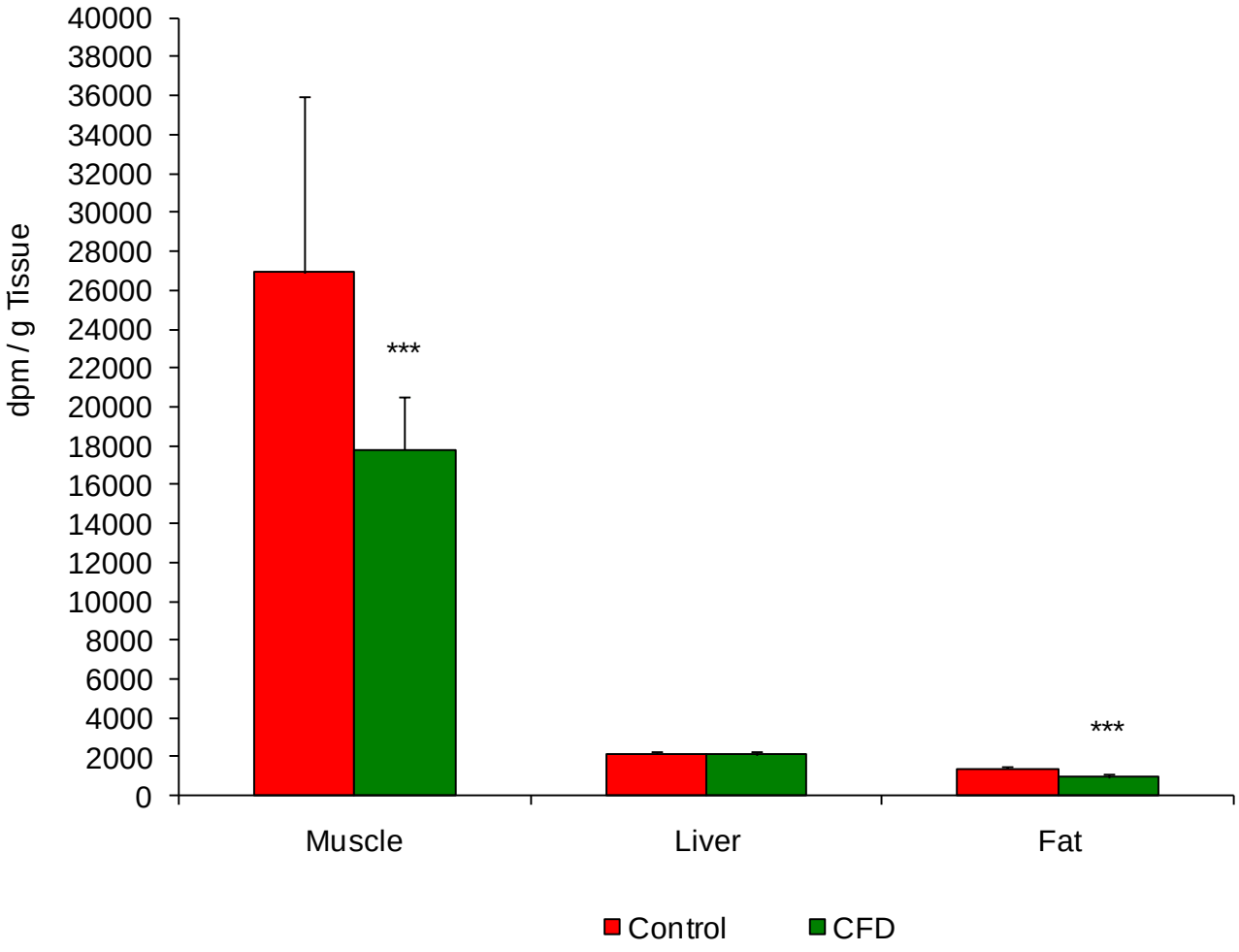

Figure 18: 2-deoxy-[^{3}H]-D-glucose uptake in muscle, liver and fat tissue at three months

Values are expressed as mean ± SD. Muscle: CFD vs. control, *** p=0.0008; Fat: CFD vs. control, *** p<0.0001.

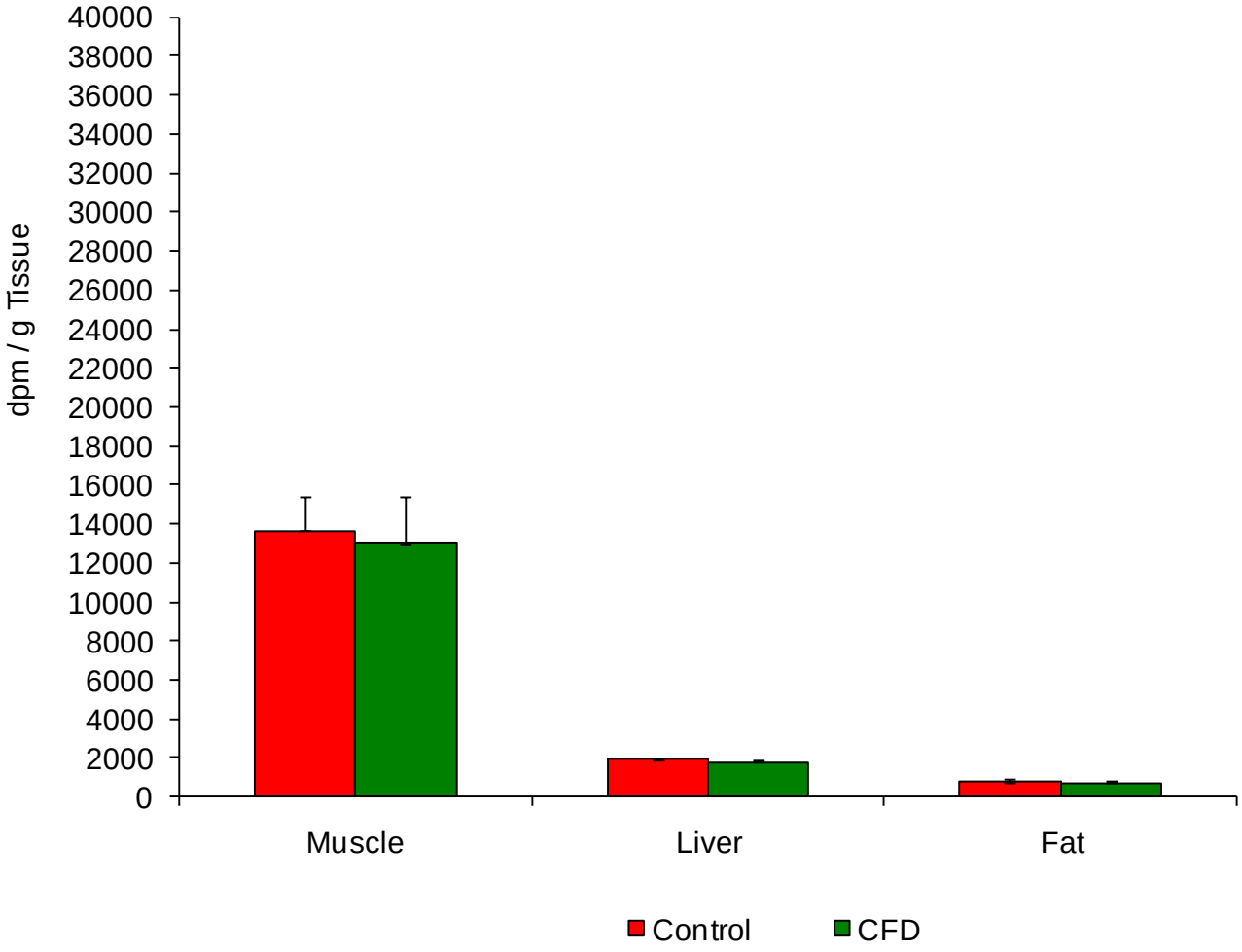

Figure 19: 2-deoxy-[^{3}H]-D-glucose uptake in muscle, liver and fat tissue at twelve months

Values are expressed as mean ± SD. $p>0.05$ between groups.

3.7 IHC staining of pancreatic sections

3.7.1.1 Double immunolabeling for glucagon and insulin

Double immunolabeling for glucagon and insulin revealed the typical endocrine arrangement of α-cells at the periphery of the islets and the more abundant β-cells in the centre of the islets. Method controls Fig. 20 were employed to verify the specificity of the immunostaining.

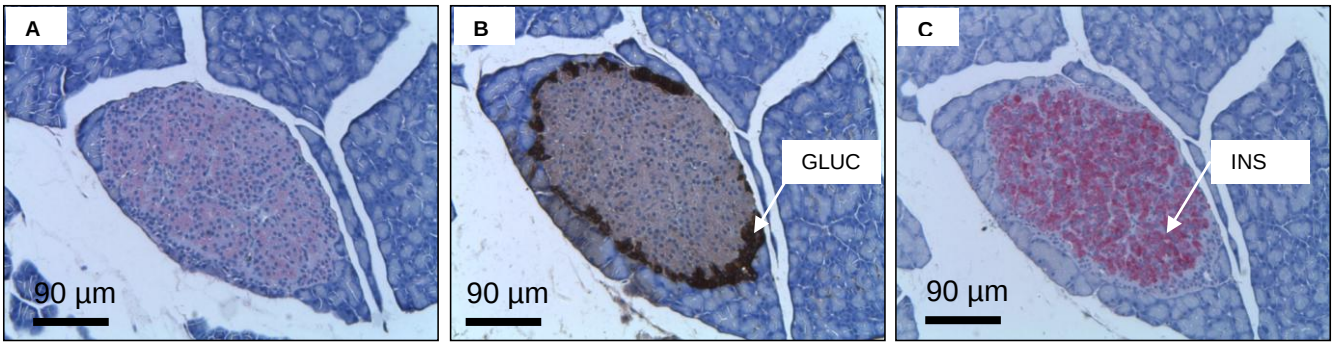

Original magnification x 100.

Figure 20: Photomicrographs of IHC method controls

Low levels of non-specific background staining were detected using method controls in which both primary antibodies were omitted (A). Method controls verified the specificity of glucagon IHC staining by omitting insulin antibody (B), and insulin specificity by omitting glucagon antibody (C).

3.7.1.2 Islet morphology

The islet morphology double immunostaining for insulin (red) and glucagon (brown) at three months showed that the islets were morphologically unaffected by the diets (Fig 21). However, at twelve months the islets of rats fed a HFD and CFD showed an increased appearance of hypertrophied irregular islets. In the CFD fed rats, the large irregular islets showed an increased presence of amorphous deposits and fibrous changes (Fig 21).

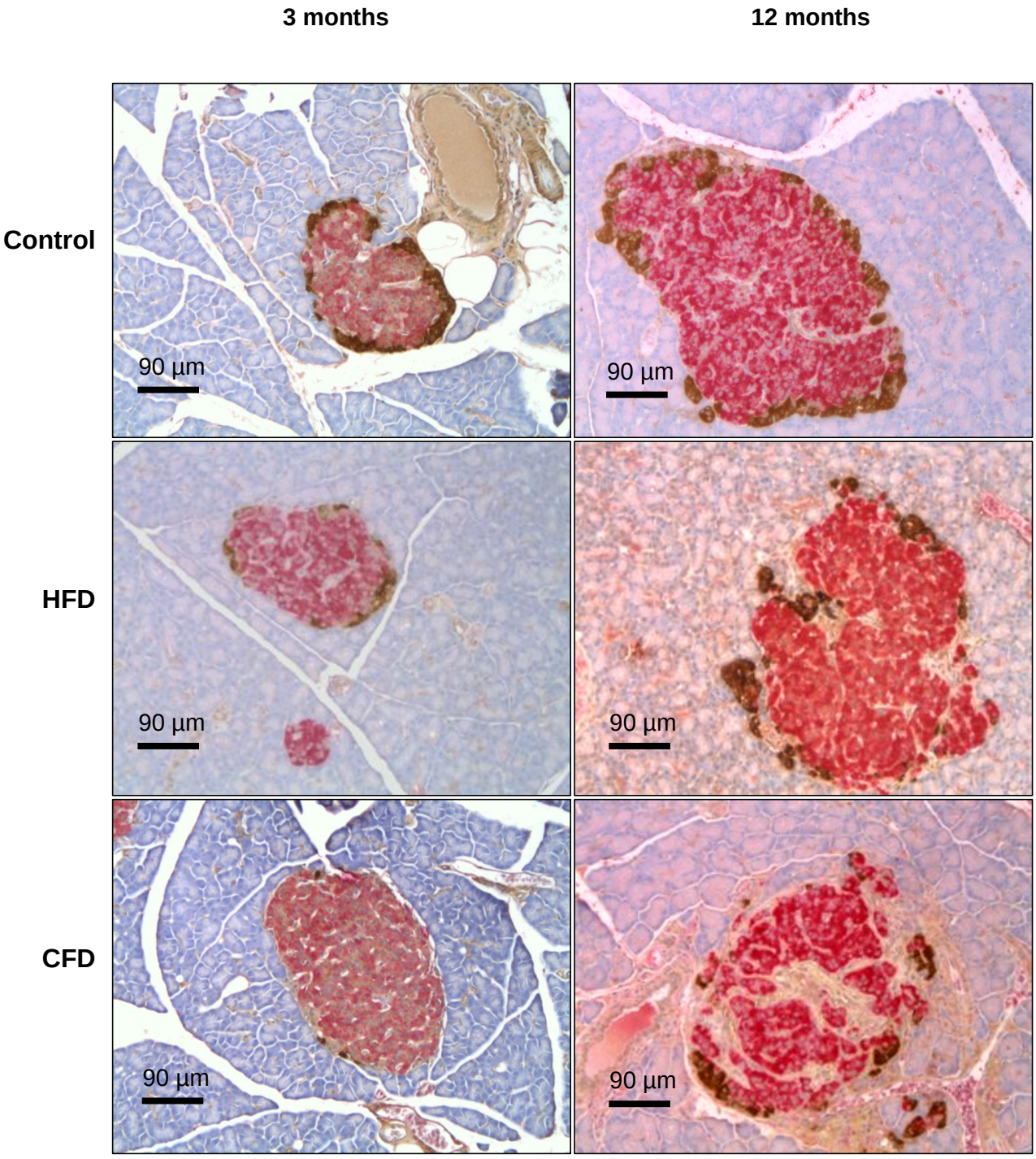

Original magnification x 100.

Figure 21: Photomicrographs of islets at three and twelve months

IHC staining of β-cells using an anti-insulin antibody stained red and the brown staining indicates the α-cells demonstrated by anti-glucagon antibody binding.

3.7.2 Morphometrical parameters

There were no significant differences measurable at three months on the diets compared to the controls. Morphometrical parameters showed significant increases in the endocrine/exocrine area and body mass to β-cell/exocrine ratio of the CFD and HFD vs. controls at twelve months (Table 10). The β-cell/α-cell ratio of the CFD was also increased compared to controls at twelve months (Table 10).

In the HFD and CFD at twelve months the percentage of small islets (<2500 μm²) increased relative to the three months with a concomitant decrease in larger islets (20 001-99 999 μm²) (Table 11 and Fig 22a and Fig 22b).

Table 10: Morphometrical parameters at three and twelve months

Morphometrical parameters		Mean islet size (μm^2)	Endocrine/exocrine area	β-cell/ α-cell ratio	Body mass to β-cell/ exocrine ratio
3 months	Control	50067 ± 17698	0.008 ± 0.003	0.62 ± 0.03	1.90 ± 0.71
	HFD	76331 ± 46058	0.013 ± 0.006	0.60 ± 0.08	3.68 ± 1.91
	CFD	62014 ± 26175	0.012 ± 0.006	0.66 ± 0.06	4.1 ± 2.23
12 months	Control	56913 ± 38272	0.011 ± 0.002	2.17 ± 0.42	2.64 ± 1.10
	HFD	36493 ± 25875	0.029 ± 0.008*	5.21 ± 2.37	10.29 ± 4.06**
	CFD	37277 ± 22788	0.029 ± 0.010*	7.10 ± 3.87*	7.45 ± 1.94*

Values are expressed as mean ± SD. CFD vs. control, * p<0.05; HFD vs. control, * p<0.05; ** p<0.001.

Table 11: Percentage islet distribution between diets at three and twelve months

Percentage islet distribution	Control		HFD		CFD	
	3 months	12 months	3 months	12 months	3 months	12 months
<2500 µm²	28 ± 16	33 ± 23	23 ± 8	43 ± 18 *	22 ± 10	49 ± 13 **
2501 – 7500 µm²	18 ± 7	16 ± 1	18 ± 5	20 ± 7	16 ± 6	20 ± 4
7501-12500 µm²	10 ± 2	8 ± 5	9 ± 4	8 ± 5	10 ± 2	5 ± 4 †
12501-20000 µm²	7 ± 4	7 ± 4	7 ± 5	6 ± 4	6 ± 4	5 ± 2
20001-99999 µm²	21 ± 9	22 ± 10	28 ± 7	15 ± 7 †	32± 6	12 ± 4 †††
>100000 µm²	15 ± 9	15 ± 11	16 ± 6	8 ± 3 †	14 ± 5	9 ± 5

Values are expressed as mean ± SD. * vs. three months of the same islet size and diet ; † vs. twelve months of the same islet size and diet; * $p \leq 0.05$; ** $p \leq 0.001$; †; $p \leq 0.05$;†††; $p<0.0001$.

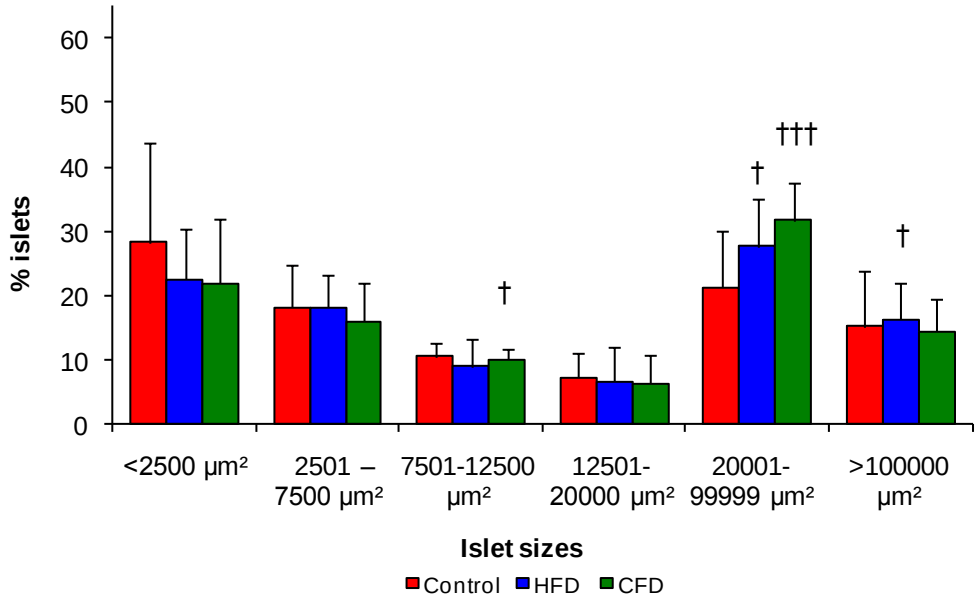

Figure 22a: Percentage islet distribution at three months

Values are expressed as mean ± SD. † vs. twelve months of the same islet size and diet; † p ≤0.05 ;††† p<0.0001.

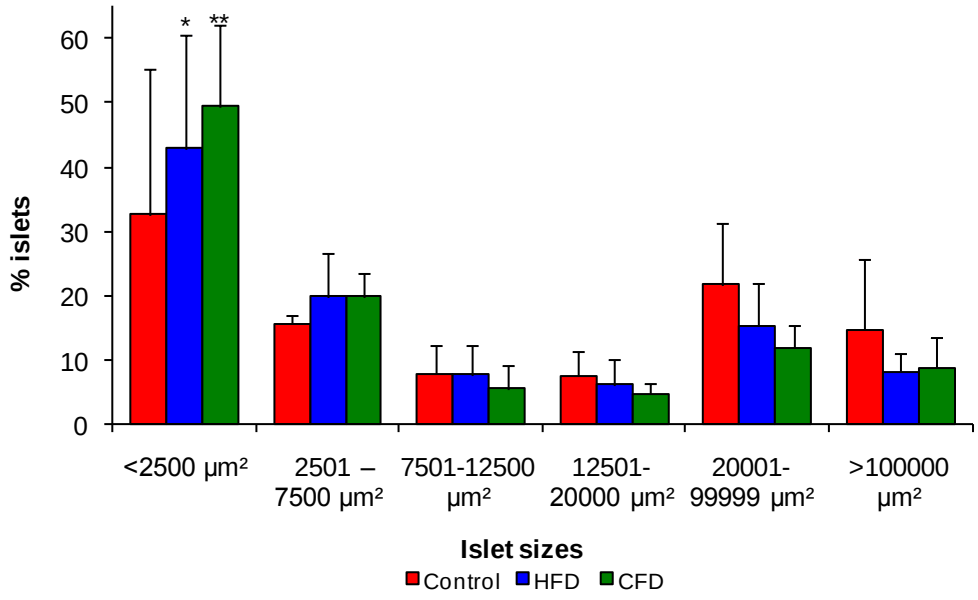

Figure 22b: Percentage islet distribution at twelve months

Values are expressed as mean ± SD. * vs. three months of the same islet size and diet * p ≤0.05; ** p ≤ 0.001.

3.7.3 GLUT2 image analyses

The staining intensity of the different diets at three months showed no difference between diets although at twelve months the CFD GLUT2 images appeared more intense when compared to the controls and HFD (Fig 23). Scoring of GLUT2 immunohistochemical staining intensity by two independent blinded scorers showed that there was no difference in the GLUT2 staining intensity of the pancreatic islets between the diet groups at three months (control: 2.3 ± 0.48 vs. HFD: 2.4 ± 0.52 vs. CFD: 2.7 ± 0.48) (Table 12). At twelve months the GLUT2 staining intensity of the CFD fed rats was increased compared to the controls (control: 1.7 ± 0.67 vs. CFD: 2.6 ± 0.53, p=0.02) (Table 12).

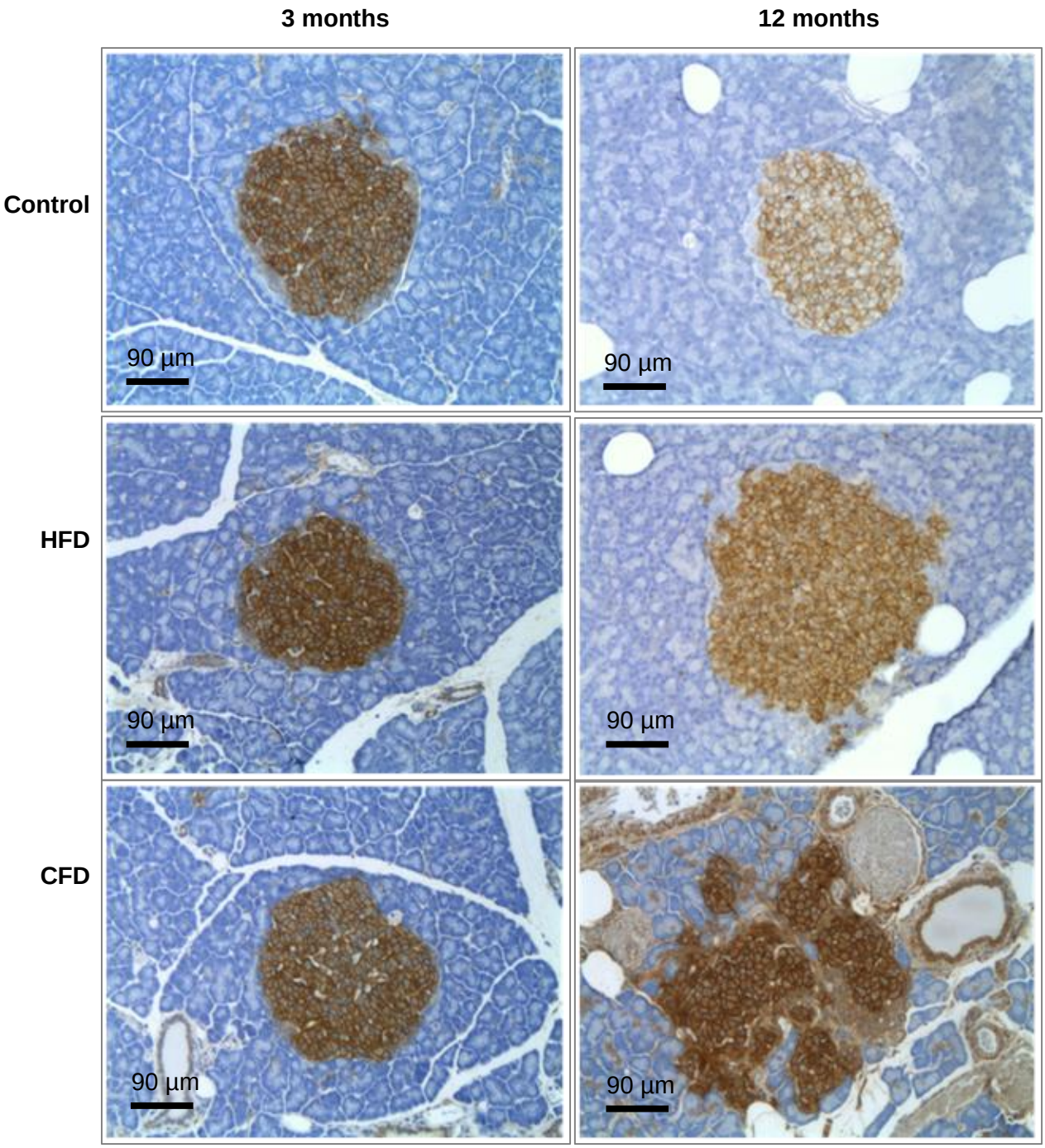

Original magnification x 100.

Figure 23: GLUT2 pancreatic immunostaining

Plasma membrane GLUT2 of the pancreatic islets is visualized by DAB immunostaining (brown).

Table 12: Evaluation of GLUT2 staining

GLUT2 scoring		
3 months	**Control**	2.3 ± 0.48
	HFD	2.4 ± 0.52
	CFD	2.7 ± 0.48
12 months	**Control**	1.7 ± 0.67
	HFD	1.8 ± 0.79
	CFD	2.6 ± 0.52 *

Values expressed as mean ± SD. CFD vs. control, * p=0.02.

3.7.4 MIB5 and Insulin immunostaining

The MIB5 staining in all diets at three and twelve months was very low (< 5%) or no staining at all. Few detectable MIB5 positive β-cells were observed at three months in all three groups although this was < 5% (Table 13). In the CFD rats at twelve months there were also few positive β-cells with no detection in HFD and control rats.

Table 13: Evaluation of MIB5 and insulin staining

MIB5 scoring		
3 months	**Control**	0.60 ± 0.55
	HFD	1.00 ± 0.00
	CFD	0.80 ± 0.45
12 months	**Control**	0.00 ± 0.00
	HFD	0.00 ± 0.00
	CFD	0.60 ± 0.55

Values expressed as mean ± SD.

3.8 Electron micrographs of CFD at twelve months

Electron micrographs confirmed the appearance of degenerative changes in the pancreas tissue of rats fed CFD for twelve months also the presence of fibrous tissue, macrophages and inflammatory cells (Figures 24a and 24b).

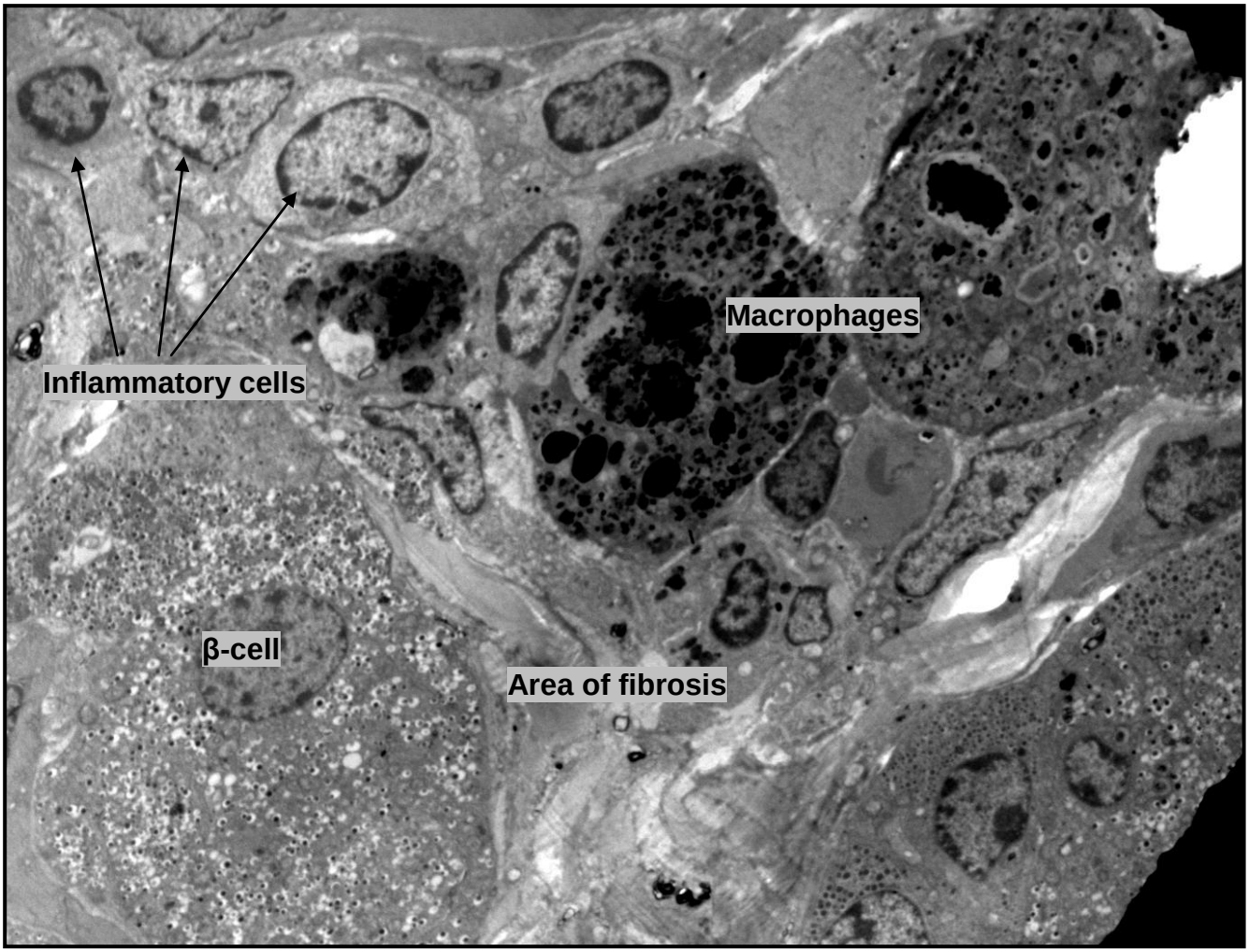

Original magnification x 2000.

Figure 24a: Electron micrograph of a pancreatic islet at twelve months on CFD

The presence of β-cells (left and right lower corner), areas of fibrous and the presence of various inflammatory cells including lymphocytes and macrophages can be seen within the islet.

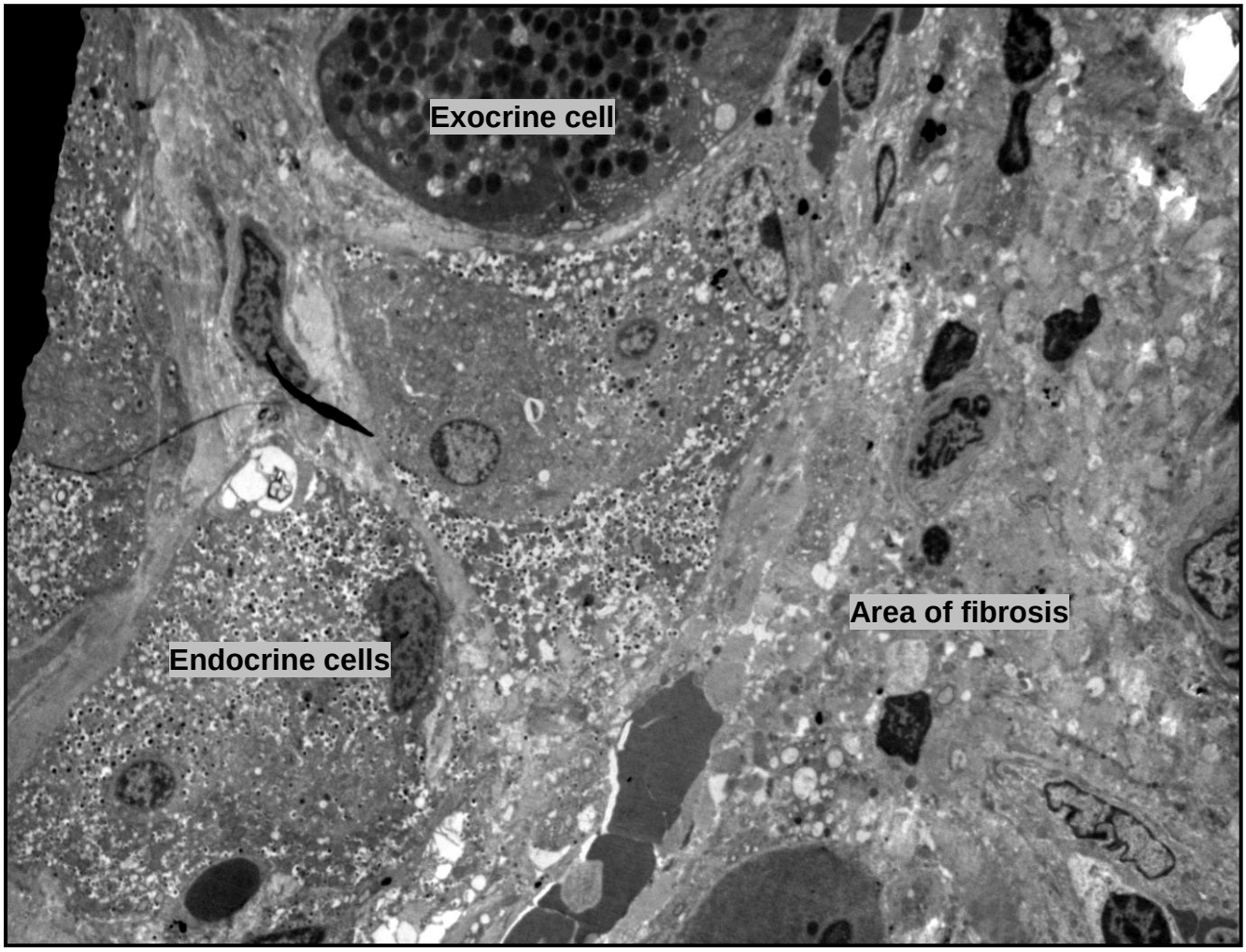

Original magnification x 2500.

Figure 24b: Electron micrograph of a pancreatic tissue of CFD fed rat at twelve months

Endocrine cells and an exocrine cell (top) with a large area of fibrosis (left) can be seen.

SUMMARY OF RESULTS

Table 14: Summary of results

Parameters		3 months		12 months	
		HFD	CFD	HFD	CFD
Calorific intake		↑	↑	↑	↑
Body weight		↑	↑	↑	↑
RF weight		↑	↑	↑	↑
Fasting glucose		no change	no change	no change	↑ (controls and HFD)
Fasting insulin		no change	↑	↓ (CFD and controls)	↑ (HFD)
HOMA-IR		no change	↑	no change	↑ (HFD and controls)
IVGTT AUC		no change	no change	no change	↑(controls and HFD
GS-ISR AUC		no change	no change	no change	↓(HFD)
2-deoxy-[^{3}H]-D-glucose uptake	**muscle**	–	↓	–	no change
	liver	–	no change	–	no change
	fat	–	↓	–	no change
Mean islet size		no change	no change	no change	no change
Endocrine/exocrine area		no change	no change	↑	↑
β-cell/α-cell ratio		no change	no change	no change	↑
Body mass to β-cell/exocrine ratio		no change	no change	↑	↑
GLUT2		no change	no change	no change	↑
MIB5/ins		no change	no change	no change	no change
Islet morphology		no change	no change	Hypertrophied irregular islets	Large irregular islets, areas of fibrosis and inflammation

All arrows indicating significance compared to controls unless stated otherwise. (↑= increased; ↓= decreased; – = not applicable)

CHAPTER FOUR

DISCUSSION

Overview

The specific diets in this study were used to compare a high-fat diet (HFD) and café diet (CFD), which combines a high-fat diet with the addition of sucrose/fructose to mimic a typical westernized diet, to a normal balanced diet (control) (Botezelli, 2010). Western diets classically include refined foods with high calorific value and a high fat content (Cerf, 2007). In addition, the increased consumption of fructose-rich corn syrup, used as sweeteners in soft drinks has further exacerbated the scourge of obesity, insulin resistance (Hofmann and Tschöp, 2009) and the development of T2D (Huang *et al*, 2004). In the USA a sharp increase in recent years in the incidence of metabolic syndrome and obesity has been positively correlated with a 30% increase in the consumption of fructose (Botezelli, 2010). In animals a fructose based diet has been shown to induce similar disturbances to lipid (Botezelli, 2010) and carbohydrate metabolism (Huang *et al*, 2004). In this study the effect of a high-fat diet in combination with fructose and sucrose were evaluated in Wistar rats after three months (mature) and twelve months (aged). This was to access the relationship between diet and age in the progression of obesity, glucose intolerance, insulin resistance and T2D.

4.1 Diet and calorific intake

During this study we showed that at three months the HFD and CFD fed rats consumed more calories than the control fed rats. Similarly, at twelve months, the HFD and CFD calorific intake was increased compared to the controls. The increase in food intake between the HFD and CFD fed rats could be due to the increased palatability of the HFD which promotes hyperphagia (Cerf, 2005) consisting of moist patties compared to the controls which received standard laboratory chow dry pellets. Diets high in saturated fats, palmitate, has been implicated as causing brain insulin resistance by a reduction in leptin and insulin signaling, which are important hormones responsible for the regulation of food intake (Benoit *et al*, 2009). Therefore this could possibly be the reason for hyperphagic effect of the HFD and CFD fed rats. Interestingly, the HFD fed rats consumed more calories than the CFD fed rats at twelve months. This was despite the increased amount of calories introduced by the addition of the sucrose/fructose to their drinking water.

4.2 Body weight and obesity

The increased 40% energy as fat, in the HFD and CFD, played a role in the increased body weight when compared to the control fed rats, which received standard diet with 10% energy as fat. Studies comparing a standard diet, of approximately 10 % energy as fat, to increasing dietary fat content have found similar results (Kamgang *et al*, 2005; Krygsman *et al*, 2010). At three and twelve months, the CFD fed rats gained more weight compared to the HFD fed rats, although this was not significant which suggests that the addition of sucrose/fructose to a HFD might have an effect on weight gain. An evaluation of the consumption of take-away foods (includes foods such as pizza, burgers, fries and fried chicken) in young adults in Australia revealed a higher prevalence of moderate abdominal obesity when eating take-away

food twice a week or more which further links the effect of high-fat diets to obesity (Smith *et al*, 2009).

No intervention for energy expenditure was applied during the study therefore these rats, due to confinement in the cages, were submitted to a sedentary lifestyle which combined with high-fat feeding further exacerbated the development of obesity (Zimmet *et al*, 2001).

As a measure of obesity, the RF pads were excised and weighed. The measurement of this adipose tissue has been previously used as a measure of body fat (de Freitas Mathias *et al*, 2007). As with the body weight, the RF pads of the CFD fed rats was increased compared to the controls. Similarly to body weight the CFD fed rats RF weights also slightly increased compared to the HFD fed rats albeit not significant. Obesity is associated with an increased number of adipocytes (Thévenod, 2008) and can lead to leptin resistance (Galic *et al*, 2010). Adipocytes produce leptin which is an appetite suppresser that has been shown to be over-produced in obese subjects (Zhang and Scarpase, 2006; Thévenod, 2008). Overproduction of leptin and cytokines, such as TNF-α and IL-6, in adipose tissue can cause cellular resistance to insulin in the adipose tissues and can also cause insulin resistance in muscle, liver (Thévenod, 2008), brain (Benoit *et al*, 2009) and lead to T2D (Galic *et al*, 2010). Leptin resistance promotes obesity which leads to further devastation of metabolic systems in the body (Zhang and Scarpase, 2006; Benoit *et al*, 2009). Saturated fatty acids especially palmitate, has been implicated in the development of brain insulin resistance by attenuated insulin activity and reduced leptin signaling in the brain hereby contributing directly to obesity (Benoit *et al*, 2009).

4.3 Fasting blood glucose and serum insulin concentrations

At three months the diets had no effect on fasting blood glucose concentrations. Suggesting that at three months the rats were able to compensate for the diabetogenic effects of the HFD and CFD. Despite maintaining normoglycemia, serum insulin concentrations at three months were increased in the CFD and were slightly increased in the HFD although this was not significant. Suga *et al* also reported substantial insulin resistance and hyperinsulinemia during fructose feeding after two weeks (Suga *et al*, 2000). The increasing insulin concentrations induced by the CFD and HFD gives an early indication of a degree of insulin resistance. In a similarly study sucrose and high-fat feeding for eight to nine weeks resulted in normoglycemia but with increased insulin concentrations (Hallfrisch *et al*, 1981) Obese individuals may exhibit normoglycemia due to the sufficient production of insulin but suffer from insulin resistance in the peripheral tissues such as muscle, liver and adipose tissue (Sesti, 2006). However, when the pancreas reaches its capacity to overproduce insulin this then leads to elevated fasting blood glucose concentrations and impaired glucose tolerance (Sesti, 2006; Thévenod, 2008).

At twelve months, the CFD fed rats developed mild hyperglycemia. The fact that the HFD fed rats did not develop hyperglycemia suggests that the Wistar rats were able to adapt to high-fat feeding and that the addition of sucrose/fructose was required to produce early signs of glucose intolerance and T2D. These findings further support the evidence that the addition of fructose enhanced sweeteners like corn syrup to food and especially soft drinks is contributing to obesity and T2D in humans (Bray *et al*, 2004; American Diabetes Association, ADA, 2006; Hofmann and Tschöp, 2009). At twelve months, fasting serum insulin concentrations of the CFD fed rats were further increased, which, together with the

hyperglycemia is clinically consistent with early T2D. In contrast the HFD and the control rats maintained normal insulin serum concentrations.

4.4 Homeostatic model assessment of insulin resistance (HOMA -IR)

The HOMA-IR model for the assessment of insulin resistance is commonly used as a tool for measuring the degree of insulin resistance. The greater the HOMA-IR value, the greater the degree of insulin resistance is for that individual (Bonora *et al*, 2002).

The HOMA-IR value of the CFD rats were increased at both three months and twelve months when compared to HFD and control fed rats. A review by Stanhope and Havel revealed increased HOMA-IR in humans consuming fructose-rich diets (Stanhope and Havel, 2009). Taken together the relationship between diet, age, glucose homeostasis and insulin sensitivity has clearly been established in this model. The addition of sucrose/fructose to a high-fat diet worsens obesity, exacerbates glucose intolerance, insulin resistance and increases the risk of developing T2D over time (Hofmann and Tschöp, 2009). The relationships between fatty acids, obesity and insulin resistance have been well established (Boden and Carnell, 2003; Boden, 2006; Krygsman *et al*, 2010). High concentrations of fructose also contribute to the development of insulin resistance. Initially, fructose was thought to be a safe low glycemic index sugar for diabetes patients as fructose does not acutely raise blood glucose concentrations (Sánchez-Lozada *et al*, 2008) nor does it stimulate insulin secretion (Elliott *et al*, 2002) as β-cells lack a fructose transporter (Elliott *et al*, 2002; Bray *et al*, 2004). Fructose is mainly transported into the cell by the insulin insensitive glucose transporter GLUT5 (Bray *et al*, 2004; Botezelli *et al*, 2010). According to the ADA, diabetes patients should avoid the

use of fructose sweeteners. However, small amounts such as present in fruits and vegetables, has very minimal effect on glucose metabolism as it usually only accounts for approximately 3-4% of energy intake (ADA, 2006). At high concentrations, as was in our CFD diet most of the fructose is converted to fatty acids in the liver and this further exacerbates insulin resistance (Botezelli *et al*, 2010).

4.5 Intravenous glucose tolerance test, glucose stimulated insulin secretion and glucose clearance rate

Intravenous glucose administration was preferred as it elicits tissue response to glucose uptake particularly in muscle then liver and fat. Interference that may occur as a result of gastrointestinal tract glucose uptake is reduced (DeFronzo, 2004).

At three months the respective diets had no effect on the glucose concentrations after glucose stimulation at any of the time points. Similar results were obtained in a study on normal diet versus increasing amounts of high-fat diets over two months (Krygsman *et al*, 2010). However, the IVGTT AUC value was higher in CFD rats compared to HFD and controls although this was not significant. The GCR of the HFD and CFD fed rats was also diminished indicating defective clearance of glucose from the circulation.

By twelve months the CFD fed rats had increased peak glucose concentrations at 3, 5 and 10 min after glucose stimulation. The AUC values of the CFD fed rats increased compared to the HFD and control fed rats. The GCR rates of the HFD and CFD fed rats had deteriorated further compared to the three month values. These results show an age related progression in glucose intolerance following an IVGTT. Similarly in a review by DeFronzo (2004) where rheses monkeys presented with decreased tissue sensitivity to insulin. When aged, a high

percentage of these monkeys developed T2D (DeFronzo, 2004). Glucose stimulated-insulin secretion rates, at three months, showed a trend towards increased serum insulin peak values at 5 and 10 min in the CFD rats and increased AUC values when compared to HFD and controls. By twelve months the GS-ISR insulin concentrations of the CFD rats were reduced at 30 min compared to the HFD and the control fed rats. An overall reduction in the insulin response to the glucose bolus was observed over the one hour period. As was reflected in the lower AUC values compared to the control and HFD fed rats. The IVGTT and GS-ISR studies showed that CFD fed rats developed glucose intolerance and initial insulin resistance at three months. By twelve months the diet induced affects had progressed into an insulin deficient response to glucose stimulation resulting in loss of glucose control.

Concurring to our finding in two months old rats infused with glucose and fat emulsion in Wistar rats showed no effect on insulin sensitivity or insulin secretion suggesting that glucolipotoxicity has no effect in young Wistar rats (Fontés *et al*, 2010). The same study also evaluated six months old rats and which showed reduced glucose-induced insulin secretion (Fontés *et al*, 2010).

4.6 2-deoxy-[^{3}H]-D-glucose uptake in muscle, liver and fat tissue

Deoxy-glucose is taken up by tissue in the body at the same rate as glucose (Utriainen *et al*, 2000). The deoxy-glucose is however, not metabolized by the cells therefore accumulates intra-cellularily (Chadwick *et al*, 2007). Therefore radio-active labeled 2-deoxy-[^{3}H]-D-glucose can serve as a tool in measuring glucose uptake (Chadwick *et al*, 2007). The route of glucose administration to the body also plays a major part in glucose uptake (DeFronzo,

2004). During intravenous glucose administration, the majority of glucose is disposed of by the muscle tissues (approximately 80-90%) and to a lesser extent the liver and fat tissue (DeFronzo, 2004).

Glucose uptake as measured by 2-deoxy-[^{3}H]-D-glucose in the three months fed a CFD, rats showed reduced glucose uptake in the muscle and fat tissue. The reduction in glucose uptake of muscle and fat is consistent with peripheral insulin resistance and the subsequent failure of these insulin sensitive tissues to clear glucose from the circulation. By twelve months there were no differences in labeled glucose uptake between diet groups. This was interesting, but not an unexpected finding, as with age, increasing levels of glucose intolerance occurs in sedentary animals (Tokuyama and Suzuki, 1998) which was demonstrated in decreased GCR of all three the diet groups at twelve months. An overall reduction in muscle glucose uptake was observed at twelve months when compared to three months which further suggest an age-related decrease in glucose disposal in muscle.

4.7 Islet morphometry of pancreatic tissue

4.7.1 Immuno-labeled insulin and glucagon

Pancreas tissue was immuno-stained for insulin and glucagon which revealed the β-cells and α-cells respectively. This method was used to identify the pancreatic islets as the β-cells and α-cells constitute approximately 95% of the islet endocrine cells. At three months, in terms of islet morphology, no diet induced effect could be observed between the groups. At twelve months, however, diet had a profound effect on the morphology of especially the larger islets. In the HFD group, the morphological changes were limited to the larger islets that appeared

more irregular and lobular. These irregularly shaped islets also showed signs of segregation of endocrine islet component by fibrous tissue. In CFD group, at twelve months, these morphological changes were more profound with an increase in intra-islet fibrous tissue deposition and complete segregation of the islet into smaller sub-islets. Furthermore the arrangement of the endocrine cells within these affected islets appeared to be more cord-like which suggest that the normal glomus like vascular arrangement was disrupted. Although no morphological changes were observed at three months, morphometry revealed an increase in the percentage of larger islets in the HFD and CFD groups. The increase in the proportion of larger islets is consistent with a diet induced hypertrophic compensatory process. At twelve months, in contrast to three months, morphometry revealed that the incidence of smaller islets had increased. This would suggest that the diet induced adaptive process had changed from a hypertrophic to hyperplastic. Perhaps the demise of the larger islets could be partial proof of compensatory response by increased amount of smaller islets which could indicate new islet formation. In addition, there was an increase in the islet area per pancreas and an increase in β-cell area per islet. This confirms that the β-cells of the HFD and CFD rats were still able to adapt to the dietary and metabolic demand at twelve months. This is a surprising finding as Wistar rats are regarded to be mature at two to three months and aged at 14.5 to 15.5 months (Biagas *et al*, 1996) and it is generally accepted that β-cell regeneration diminishes with age (Bouwens and Rooman, 2006).

4.7.2 Immunostaining of GLUT2

GLUT2 immunostaining was performed on pancreas tissue of respective diets at three and twelve months. Immunostaining of GLUT2 at three months revealed no significant difference in staining between CFD, HFD and control fed rats. At twelve months the staining intensity

was reduced in the HFD and controls when compared to the three months group. This is an indication that in β-cells, GLUT2 expression is regulated or affected by diet and in particular our CFD fed rats. This finding is in line with a study by Gouyon *et al*, 2003, where massive recruitment of GLUT2 occurs upon ingestion of a simple sugar rich meal.

4.7.3 Double immuno-labeling of MIB5 and insulin

MIB5/Insulin double-immunolabeling was also performed on pancreatic sections from the diets to detect proliferating β-cells which stain positive for both MIB5 and insulin. In this study very few MIB5/insulin positive β-cells were detected with no significant difference among all diet groups at three and twelve months of the study. However, the CFD fed rats showed a non-significant increase in proliferating β-cells in comparison to the control diet rats at three and twelve months. This further supports the findings that in Wistar rats β-cell adaptation to dietary stimulation occurs for up to twelve months.

4.8 Electron microscopy

Electron microscopy confirmed the light microscopical observations and in addition revealed the presence of an active inflammatory process with the presence of lymphocytes and macrophages laden with residual bodies. The presence of these inflammatory cells, usually characteristic of T2D, together with the islet fibrous changes is suggestive of chronic inflammation (de Koning *et al*, 2008). It is of interest that the changes were limited to the larger islets. The logical conclusion would be that these islets are older and therefore have been subjected to the diet for a longer period or they have been more active and therefore more susceptible to oxidative stress. Taken together the morphological changes and the

presence of inflammatory processes are consistent with T2D (Zozulinska and Wierusz-Wysocka, 2006).

CHAPTER FIVE

CONCLUSION

CONCLUSION

High-fat diet fed to Wistar rats increased body weight and lead to increased abdominal adiposity. The addition of sucrose/fructose to a high-fat diet exacerbated insulin resistance and glucose intolerance. The dietary period (three or twelve months) together with ageing of the rats further contributed to the advancement of insulin resistance to hyperglycemia. In agreement with other studies, the twelve months HFD and CFD fed rats did not present with overt signs of T2D. However, in this study at twelve months morphological changes in the larger islets were consistent with the development of T2D. Interestingly, despite the degenerative changes in the larger size islets of the HFD and CFD fed rats, there was an increase in the proportion of small islets. This would suggest that despite long-term insulin resistance, glucose intolerance and reduced peripheral glucose disposal, β-cell compensatory mechanism/s still occurred in aged Wistar rats.

SHORTCOMINGS AND FUTURE PROSPECTS

Palatability of dry pellets and moist patty diets should be considered in future study design and dry pellets substituted by moist patties.

The use of metabolic cages for determination of twenty four hour urine and stool production, and food and water intake. Analysis of biochemical electrolytes in the urine can be measured (e.g. ketones, urea and creatinine).

The pancreas was not weighed therefore parameters such as β-cell mass could not be determined.

Liver should be assessed for histopathological changes associated with T2D such as steatosis and fibrosis.

Demonstrate β-cell apoptosis using antibodies such as BAX, caspase3 or tunnel.

Determine serum free fatty acid profile thereby establishing the effect of specific free fatty acids on insulin resistance. Assess inflammatory status of the rats like TNF-α and IL-6 using enzyme-linked immunosorbent assays (ELISA).

To determine the dietary effect on insulin signaling in muscle, liver and fat thereby establishing a molecular basis for the insulin resistance.

Ex-vivo studies on isolated β-cells to assess the functional capacity of the islets following dietary insult.

REFERENCES

American Diabetes Association (ADA): Nutrition recommendations and interventions for diabetes–2006. *Diabetes Care* 2006; 29 (9): 2140-2157.

Araujo EP, Amaral ME, Filiputti E, De Souza CT, Laurito TL, Augusto VD, Saad MJ, Boschero AC, Velloso LA and Carneiro EM. Restoration of insulin secretion in pancreatic islets of protein-deficient rats by reduced expression of insulin receptor substrate (IRS)-1 and IRS-2 *Journal of Endocrinology* 2004; 181: 25-38.

Azevedo A, Santos AC, Ribeiro L and Azevedo I. The metabolic syndrome. In R Soares and C Costa (Eds), *Oxidative Stress, Inflammation and Angiogenesis in the Metabolic Syndrome* 2009; 1-19.

Basciano H, Federico L and Adeli K. Fructose, insulin resistance, and metabolic dyslipidemia. *Nutrition and Metabolism* 2005; 2 (1): 5-18.

Benoit SC, Kemp CJ, Elias CF, Abplanalp W, Herman JP, Migrenne S, Lefevre A, Cruciani-Guglielmacci C, Magnan C, Yu F, Niswender K, Irani BG, Holland WL, and Clegg DJ. Palmitic acid mediates hypothalamic insulin resistance by altering PKC-θ subcellular localization in rodents. *The Journal of Clinical Investigation* 2009; 119 (9): 2577- 2589.

Biagas KV, Grundl PD, Kochanek PM, Schiding JK and Nemoto EM. Post-traumatic hyperemia in immature, mature, and aged rats: autoradiographic determination of cerebral blood flow. *Journal of Neurotrauma* 1996; 13 (4): 189-200.

Boden G. Obesity, insulin resistance, type 2 diabetes and free fatty acids. *Expert Review of Endocrinology and Metabolism* 2006; 499-507.

Boden G and Carnell LH. Nutritional effects of fat on carbohydrate metabolism. *Best Practice and Research. Clinical Endocrinology and Metabolism* 2003; 17 (3): 399-410.

Bonner-Weir S and Weir GS. New sources of pancreatic β-cells. *Nature Biotechnology* 2005; 23: 857-861.

Bonora E, Formentini G, Calcaterra F, Lombardi S, Marini F, Zenari L, Saggiani F, Poli M, Perbellini S, Raffaelli A, Cacciatori V, Santi L, Targher, Bonadonna R and Muggeo M. HOMA-estimated insulin resistance is an independent predictor of cardiovascular disease in type 2 diabetic subjects. *Diabetes Care* 2002; 25: 1135-1141.

Botezelli JD, Dalia RA, Reis IM, Barbieri RA, Rezende TM, Pelarigo JG, Codogno J, Gonçalves R and Mello MA. Chronic consumption of fructose rich soft drinks alters lipids of rats. *Diabetology and Metabolic Syndrome* 2010; 2 (1): 43-50.

Bouwens L and Rooman I. Regulation of pancreatic beta-cell mass. *Physiological Reviews* 2005; 85: 1255–1270.

Bray GA, Nielsen SJ and Popkin BM. Consumption of high-fructose corn syrup in beverages may play a role in the epidemic of obesity. *The American Journal of Clinical Nutrition* 2004; 79: 537-543.

Buettner R, Parhofer KG, Woenckhaus M, Wrede CE, Kunz-Schughart LA, Schölmerich J and Bollheimer LC. Defining high-fat-diet rat models: metabolic and molecular effects of different fat types. *Journal of Molecular Endocrinology* 2006; 36: 485-501.

Butler AE, Jansen J, Bonner-Weir S, Ritzel R, Rizza RA and Butler PC. Beta-cell deficit and increased beta-cell apoptosis in humans with type 2 diabetes. *Diabetes* 2003; 52: 102-110.

Cerf ME, Williams K, Nkomo XI, Muller CJ, Du Toit DF, Louw J and Wolfe-Coote SA. Islet cell response in the neonatal rat after exposure to a high-fat diet during pregnancy. *American Journal of Physiology. Regulatory, Integrative and Comparative Physiology* 2005; 288: R1122-R1128.

Cerf ME, Muller CJ, Du Toit DF, Louw J and Wolfe-Coote SA. Hyperglycaemia and reduced glucokinase expression in weanling offspring from dams maintained on a high-fat diet. *British Journal of Nutrition* 2006; 95: 391-396.

Cerf ME. High fat diet modulation of glucose sensing in the β-cell. *Medical Science Monitor* 2007; 13 (1): 13-17.

Chadwick WA, Roux S, van der Venter M, Louw J and Oelofsen W. Anti-diabetic effects of *Sutherlandia frutescens* in Wistar rats fed a diabetogenic diet. *Journal of Ethnophamocology* 2007; 109: 121-127.

Chakraborty C. Biochemical and molecular basis of insulin resistance. *Current Protein and Peptide Science* 2006; 7: 113-121.

Chalkley SM, Hettiarachchi M, Chisholm DJ and Kraegen EW. Long-term high-fat feeding leads to severe insulin resistance but not diabetes in Wistar rats. *American Journal of Physiology, Endocrinology and Metabolism* 2002; 282: 1231-1238.

Chang AM, Smith MJ, Bloem CJ, Galecki AT, Halter JB and Supiano MA. Limitation of the homeostasis model assessment to predict insulin resistance and β-cell dysfunction in older people. *The Journal of Clinical Endocrinology and Metabolism* 2006; 91 (2): 629-634.

Choi K and Kim YB. Molecular mechanism of insulin resistance in obesity and type 2 diabetes. *The Korean Journal of Internal Medicine* 2010; 25: 119-129.

De Freitas Mathias PC, Grassiolli S, Rocha DN, Scomparin DX and Gravena C. Transplantation of pancreatic islets from hyperthalamic obese rats corrects hyperglycemia of diabetic rats. *Transplantation Proceedings* 2007; 39: 193-195.

De Villiers C. Standard operating procedures rodent section. Primate Unit, Technology and business development directorate, Medical Research Council 2007.

DeFronzo R. Pathogenesis of type 2 diabetes mellitus. *Medical Clinics of North America* 2004; 88: 787-835.

DeFronzo R. Overview of newer agents: where treatment is going. *The American Journal of Medicine* 2010; 123: S38-S48.

de Koning EJP, Bonner-Weir S and Rabelink TJ. Preservation of β-cell function by targeting β-cell mass. *Trends in Pharmacological Sciences* 2008; 29 (4): 218-227.

Després JP and Lemieux. Abdominal obesity and metabolic syndrome. *Nature* 2006; 444: 881-887.

Dor Y, Brown J, Martinez OI and Melton DA. Adult pancreatic beta-cells are formed by self duplication rather than stem-cell differentiation. *Nature* 2004; 429: 41-46.

Elliott SS, Keim NL, Stern JS, Teff K, and Havel PJ. Fructose, weight gain, and the insulin resistance syndrome. *The American Journal of Clinical Nutrition* 2002; 76: 911-922.

Fontés G, Zarrouki B, Hagman DK, Latour MG, Semache M, Roskens V, Moore PC, Prentki M, Rhodes CJ, Jetton TL and Poitout V. Glucolipotoxicity age-dependently impairs beta cell function in rats despite a marked increase in beta cell mass. *Diabetologia* 2010; 53 (11): 2369-2379.

Freemantle N, Holmes J, Hockey A and Kumar S. How strong is the association between abdominal obesity and the incidence of type 2 diabetes. *International Journal of Clinical Practice* 2008; 62 (9): 1391-1396.

Fujitani Y, Ueno T and Watada H. The role of pancreatic beta-cell autophagy in health and diabetes. *American Journal of Physiology-Cell Physiology* 2010; 299 (1): C1-C6.

Fulop T, Tessier D and Carpentier A. The Metabolic Syndrome. *Pathologie Biologie* 2006; 54: 375-386.

Galgani JE, Moro C and Ravussin E. Metabolic flexibility and resistance. *American Journal of Physiology, Endocrinology and Metabolism* 2008; 295: E1009-E1017.

Galic S, Oakhill JS and Steinberg GR. Adipose tissue as an endocrine organ. *Molecular and Cellular Endocrinology* 2010; 316 (2): 129-139.

Ganong WF. Endocrine functions of the pancreas and the regulation of carbohydrate metabolism. *Review of Medical Physiology* 1989; 14: 280-300.

Griffin ME, Marcucci MJ, Cline GW, Bell K, Barucci N, Lee D, Goodyear LJ, Kraegen EW, White MF and Shulman GI. Free fatty acid-induced insulin resistance is associated with activation of protein kinase cθ and alterations in the insulin signaling. *Diabetes* 1999; 48: 1270-1274.

Gouyon F, Callaud L, Carriére V, Klein C, Dalet V, Citadelle D, Kellett GL, Thorens B, Leturque A and Brot-Leroche E. Simple-sugar meals target GLUT2 at enterocyte apical membranes to improve sugar absorption: a study in GLUT2-null mice. *The Journal of Physiology* 2003; 552 (3): 823-832.

Halban PA. Cellular sources of new pancreatic beta-cells and therapeutic implications for regenerative medicine. *Nature Cell Biology* 2004; 6: 1021-1025.

Hallfrisch J, Cohen L and Reiser S. Effects of feeding rats sucrose in a high fat diet. *The Journal of Nutrition* 1981; 111: 531-536.

Hofmann SM and Tschöp MH. Dietary sugars: a fat difference. *The Journal of Clinical Investigation* 2009; 119 (5): 1089-1092.

Huang BW, Chiang MT, Yao HT and Chiang W. The effects of high-fat and high-fructose diets on glucose tolerance and plasma lipid and leptin in rats. *Diabetes, Obesity and Metabolism* 2004; 6 (2): 120-126.

Jorda M, Ghorab Z, Fernandez G, Nassiri M, Hanly A and Mehrdad Nadji M. Low nuclear proliferative activity is associated with nonmetastatic islet cell tumors. *Archives of Pathology and Laboratory Medicine* 2003; 127: 196-199.

Kahn SE, Hull RL and Utzschneider KM. Mechanisms linking obesity to insulin resistance and type 2 diabetes. *Nature* 2006; 444 (14): 840-846.

Kamgang R, Mboumi RY, Mengue N'dillé GPR and Yonkeu JN. Cameroon local diet-induced glucose intolerance and dyslipidemia in the adult Wistar rat. *Diabetes Research and Clinical Practice* 2005; 69: 224-230.

Kang ES, Yun YS, Park SW, Kim HJ, Ahn CH, Song YD, Cha BS, Lim SK, Kim KR and Lee HC. Limitation of the validity of the homeostasis model assessment as an index of insulin resistance in Korea. *Metabolism Clinical and Experimental* 2005; 54: 206-211.

Kanter Y, Kol S and Wiener F. Intravenous glucose tolerance test in gestational diabetes and pregnancy: 'manual' versus computerized assessment. *European Journal of Obstetrics, Gynecology and Reproductive Biology* 1988; 27 (4): 307-311.

Karaca M, Magnan C and Kargar C. Functional pancreatic beta-cell mass: involvement in type 2 diabetes and therapeutic intervention. *Diabetes and Metabolism* 2009; 35: 77-84.

Kellett GL and Brot-Laroche E. Apical GLUT2: A major pathway of intestinal sugar absorption. *Diabetes* 2005; 54: 3056-3062.

Kramer J, Ludlage Moeller E, Hachey A, Mansfield KG and Wachtman LM. Differential expression of GLUT2 in pancreatic islets and kidneys of New and Old World nonhuman primates. *American Journal of Physiology. Regulatory, Integrative and Comparative Physiology* 2009; 296: 786-793.

Krygsman A, Roux CR, Muller C and Louw J. Development of glucose intolerance in Wistar rats fed low and moderate fat diets differing in fatty acid profile. *Experimental and Clinical Endocrinology and Diabetes* 2010; 118 (7): 434-441.

Leturque A, Brot-Laroche E, Le Gall M, Stolarczyk and Tobin V. Role of GLUT2 in dietary sugar handling. *Journal of Physiology and Biochemistry* 2005; 61 (4): 529-538.

Leturque A, Brot-Laroche E and Le Gall M. GLUT2 mutations, translocation, and receptor function in the diet sugar managing. *American Journal of Physiology. Endocrinology and Metabolism* 2009; 296: E985-E992.

Maedler K, Sergeev P, Ris F, Oberholzer J, Joller-Jemelka HI, Spinas GA, Kaiser N, Halban PA and Donath MY. Glucose-induced β-cell production of IL-1β contributes to glucotoxicity in human pancreatic islets. *The Journal of Clinical Investigation* 2002; 110 (6): 851-860.

Marchetti P, Dotta F, Lauro D and Purrello F. An overview of pancreatic beta-cell defects in human type 2 diabetes: Implications for treatment. *Regulatory Peptide* 2008; 146: 4-11.

Monteiro S and Azevedo I. Chronic inflammation in obesity and the metabolic syndrome. *Mediators of Inflammation* 2010: 1- 10.

Pessin JE and Saltiel AR. Signaling pathways in insulin action: molecular targets of insulin resistance. *The Journal of Clinical Investigation* 2000; 106 (2): 165-169.

Pittas AG, Joseph NA and Greenberg AS. Adipocytokines and insulin resistance. *The Journal of Clinical Endocrinology and Metabolism* 2004; 89 (2): 447-452.

Prentki M and Nolan CJ. Islet β-cell failure in type 2 diabetes. *The Journal of Clinical Investigation* 2006; 116 (7): 1802-1812.

Reaven GM. Role of insulin resistance in human disease. *Diabetes* 1988; 37: 1595-1607.

Reaven GM. Why Syndrome X? From Harold Himsworth to the insulin resistance syndrome. *Cell Metabolism* 2005; 1: 9-14.

Rhodes CJ. Type 2 diabetes- a matter of beta-cell life and death? *Science* 2005; 307: 380-384.

Roglic G, Resnikoff S, Strong S and Unwin N. Report of a WHO/IDF consultation: definition and diagnosis of diabetes mellitus and intermediate hyperglycemia. World Health Organization 2006.

Sánchez-Lozada LG, Le M, Segal M and Johnson RJ. How safe is fructose for persons with or without diabetes? The *American Journal of Clinical Nutrition* 2008; 88: 1189-1190.

Santer R, Schneppenheim R, Suter D, Schaub J and Steinmann B. Fanconi-Bickel syndrome- the original patient and his natural history, historical steps leading to the primary defect, and a review of the literature. *European Journal of Pediatrics* 1998; 157 (10): 783-797.

Schröder H. Protective mechanism of the Mediterranean diet in obesity and type 2 diabetes. *Journal of Nutritional Biochemistry* 2007; 18: 149-160.

Sesti G. Pathophysiology of insulin resistance. *Best Practice and Research. Clinical Endocrinology and Metabolism* 2006; 20 (4): 665-679.

Shinohara K, Shoji T, Emoto M, Tahara H, Koyama H, Ishimura E, Miki T, Tabata T and Nishizawa Y. Insulin resistance as an independent predictor of cardiovascular mortality in patients with end-stage renal disease. *Journal of the American Society of Nephrology* 2002; 13: 1894-1900.

Smith KJ, McNaughton SA, Gall SL, Blizzard L, Dwyer T and Venn AJ. Takeaway food consumption and its associations with diet quality and abdominal obesity: a cross-sectional study of young adults. *International Journal of Behavioral Nutrition and Physical Activity* 2009; 6 (1): 29-41.

Speakman JC, Hambly C, Mitchell S and Król E. Animal models of obesity. *Obesity Reviews* 2007; 8 (1): 55-61.

Srinivasan K and Ramaroa P. Animals models in type 2 diabetes research: An overview. *The Indian Journal of Medical Research* 2007; 125 (3): 451-472.

Stanfield P and Hui YH. Carbohydrates and fats: Implications for health. *Nutrition and diet therapy: Self- Instructional Approaches* 2009; 4 (5): 47-54.

Stanhope KL and Havel PJ. Fructose consumption: considerations for future research on its effects on adipose distribution, lipid metabolism, and insulin sensitivity in humans. *The Journal of Nutrition* 2009; 139: 1236S-1241S.

Stanhope KL, Schwarz JM, Keim NL Griffin SC, Bremer AA, Graham JL, Hatcher B, Cox CL, Dyachenko A, Zhang W, McGahan JP, Seibert A, Krauss RM, Chiu S, Schaefer EJ, Ai M, Otokozawa S, Nakajima K, Nakano T, Beysen C, Hellerstein MK, Berglund L and Havel P. Consuming fructose-sweetened, not glucose-sweetened, beverages increases viseral adiposity and lipids and decreases insulin sensitivity in overweight/obeses humans. *Journal of Clinical Investigation* 2009; 119 (5): 1089-1092.

Stevens A and Lowe J. Endocrine system. *Human Histology* 2005; 3: 285-287.

Suga A, Hirano T, Kageyama H, Osaka T, Namba Y, Tsuji M, Miura M, Adachi M and Inoue S. Effects of fructose and glucose on plasma leptin, insulin and insulin resistance in lean and VMH-lesioned obese rats. *American Journal of Physiology. Endocrinology and Metabolism* 2000; 278: E667-E683.

Thévenod F. Pathophysiology of diabetes mellitus type 2: roles of obesity, insulin resistance and β-cell dysfunction, In Masur K, Thévenod F, Zänker KS (Eds), *Diabetes and Cancer* 2008; 19: 1-18.

Thorens B, Guillam MT, Beermann F, Burcelin R, and Jaquet M. Transgenic reexpression of GLUT1 or GLUT2 in pancreatic β-cells rescues GLUT2-null mice from early death and restores normal glucose-stimulated insulin secretion. *The Journal of Biological Chemistry* 2000; 275 (31): 23751-23758.

Tokuyama K and Suzuki M. Intravenous glucose tolerance test-derived glucose effectiveness in endurance-trained rats. *Metabolism* 1998; 147 (2): 190-194.

Utriainen T, Lovisatti S, Mäkimattila S, Bertoldo A, Weintraub S, DeFronzo R, Cobelli C and Yki-Järvinen H. Direct measurement of the lumped constant for 2-deoxy-[1-^{14}C] glucose *in vivo* in human skeletal muscle. *American Journal of Physiology. Endocrinology and Metabolism* 2000; 279: 228-233.

Verhelst GWC, Smagge GJ, Tirry LJ, Slegers GA and Van Peteghem CH. Determination of tritiated dexamethasone in rat liver and muscle: comparison of two sample preparation techniques, combustion and solubilization, prior to liquid scintillation counting. *Journal of Agricultural and Food Chemistry* 1998; 46: 5151-5155.

Weir GC and Bonner-Weir S. A Dominant role of glucose in β-cell compensation of insulin resistance. *The Journal of Clinical Investigation* 2007; 117 (1): 81-83.

Weir GC, Laybutt DR, Kaneto H, Bonner-Weir S and Sharma A. β-cell adaptation and decomposition during the progression of diabetes. *Diabetes* 2001; 50(1): S154-S159.

Wild S, Roglic G, Green A, Sicree R and King H. Global prevalence of diabetes. *Diabetes Care* 2004; 27 (5): 1047-1053.

Woods SC, Seeley RJ, Rushing PA, D'Alessio DD and Tso P. A controlled high-fat diet induces an obese syndrome in rats. *Journal of Nutrition* 2002; 133: 1081-1087.

World Health Organization, Obesity: Preventing and managing the global epidemic. *World Health Organization technical report series* 2000; No 894.

World Health Organization Fact sheet No. 311. September 2006. Obesity and overweight. http://www.who.int/mediacentre/factsheets/fs311/en/print.html. Date downloaded: 26/10/2010

World Health Organization Fact sheet No. 312. November 2009. Diabetes. http://www.who.int/mediacentre/factsheets/fs312/en/print.html. Date downloaded: 26/10/2010.

Yu C, Chen Y, Cline GW, Zhang D, Zong H, Wang Y, Bergeron R, Kim JK, Cushman SW, Cooney GJ, Atcheson B, White MF, Kraegen EW and Shulman GI. Mechanism by which fatty acids inhibit insulin activation of insulin receptor substrate-1 (IRS-1- associated phosphatidylinositol 3-kinase activity in muscle. *The Journal of Biological Chemistry* 2002; 227 (52): 50230-50236.

Zhang Y and Scarpase PJ. The role of leptin in leptin resistance and obesity. *Physiology and Behavior* 2006; 88: 249-256.

Zimmet P, Alberti KG, and Shaw J. Global and societal implications of the diabetes epidemic. *Nature* 2001; 414: 782-787.

Zozulinska D and Wierusz-Wysocka B. Type 2 diabetes mellitus as inflammatory disease. *Diabetes Research and Clinical Practice* 2006; 74S: S12-S16.

Zuniga FA, Shi G, Haller JF, Rubashkin A, Flynn DR, Isorovich P and Fischbarg J. A three dimentional model of the human facilitative glucose transporter GLUT1. *The Journal of Biological Chemistry* 2001; 276 (48): 44970-44975.